Copy No. 5

SC5545.FR

STUDIES OF NONLINEAR OPTICAL EFFECTS FOR AGILE BEAM STEERING

FINAL REPORT
for the period
May 1, 1988 through July 31, 1991

CONTRACT NO. N00014-88-C-0231

Prepared for:

Scientific Officer
Lasers and Optical Division
800 N. Quincy Street
Arlington, VA 22217-5000
Attn: Dr. Matthew B. White (1112LO)

Prepared by:

F. Vachss
Principal Investigator

NOVEMBER 1993

Distribution Unlimited

Rockwell International
Science Center

UNCLASSIFIED

SECURITY CLASSIFICATION OF THIS PAGE

REPORT DOCUMENTATION PAGE

FORM APPROVED
OMB No. 0704-0188

1a. REPORT SECURITY CLASSIFICATION
UNCLASSIFIED

1b. RESTRICTIVE MARKINGS

2a. SECURITY CLASSIFICATION AUTHORITY

3. DISTRIBUTION/AVAILABILITY OF REPORT
Unlimited

2b. CLASSIFICATION/DOWNGRADING SCHEDULE

4. PERFORMING ORGANIZATION REPORT NUMBER(S)
SC5545.FR

5. MONITORING ORGANIZATION REPORT NUMBER(S)

6a. NAME OF PERFORMING ORGANIZATION
ROCKWELL INTERNATIONAL
Science Center

6b. OFFICE SYMBOL (If Applicable)

7a. NAME OF MONITORING ORGANIZATION

6c. ADDRESS (City, State and ZIP Code)
1049 Camino Dos Rios
Thousand Oaks , CA 91360

7b. ADDRESS (City, State and ZIP Code)

8a. NAME OF FUNDING/SPONSORING ORGANIZATION
Office of Naval Research

8b. OFFICE SYMBOL (If Applicable)

9. PROCUREMENT INSTRUMENT IDENTIFICATION NUMBER

8C. ADDRESS (City, State and ZIP Code)
800 N. Quincy Street
Arlington, VA 22217-5000

10. SOURCE OF FUNDING NOS.

PROGRAM ELEMENT NO.	PROJECT NO.	TASK NO.	WORK UNIT ACCESSION NO.

11. TITLE (Include Security Classification)
Studies of Nonlinear Optical Effects for Agile Beam Steering

12. PERSONAL AUTHOR(S)
Vachss, F., McMichael, I., and Yeh, P.

13a. TYPE OF REPORT	13b. TIME COVERED	14. DATE OF REPORT (Year, Month, Day)	15. PAGE COUNT
Final Report	FROM 05/01/88 TO 07/31/91	1993, NOVEMBER	28

16. SUPPLEMENTARY NOTATION

17. COSATI CODES			18. SUBJECT TERMS (Continue on reverse if necessary and identify by block number)
FIELD	GROUP	SUB-GROUP	Nonlinear optics, nonlinear acousto-optics, beam steering, high power lasers.

19. ABSTRACT (Continue on reverse if necessary and identify by block number)

The objective of this program is the demonstration of a new technique for massless beam steering of high energy laser radiation. Using the effect of nonlinear electrostriction in acousto-optic devices we show large improvements in diffraction efficiency and resolution. These results are obtained through the development of a novel geometry for acousto-optic beam steering and of a prototype device designed to take advantage of this geometry. Theoretical and experimental results of this effort establish the validity of large aperture, high frequency nonlinear acousto-optic beam steering. The results are found to be applicable to steering of high power laser beams.

20. DISTRIBUTION/AVAILABILITY OF ABSTRACT
UNCLASSIFIED/UNLIMITED ☐ SAME AS RPT. ☒ DTIC USERS ☐

21. ABSTRACT SECURITY CLASSIFICATION
UNCLASSIFIED

22a. NAME OF RESPONSIBLE INDIVIDUAL

22b. TELEPHONE NUMBER (INCLUDE AREA CODE)

22c. OFFICE SYMBOL

DD FORM 1473 Previous editions are obsolete.

UNCLASSIFIED

SECURITY CLASSIFICATION OF THIS PAGE

Table of Contents

Program Summary

The goal of this program was the development of a nonlinear optical technique through which high power optical beams could be steered at high speed with high angular resolution. The high speed requirement dictates a massless beam steering technique such as that provided by acousto-optic (AO) beam deflection. The high accuracy requirement, however, additionally dictates that the system possess a large optical aperture—potentially tens of cm for space based applications. Such large apertures in standard AO beam steering systems in turn require prohibitively large acoustic driving power. In addition, the ultrasonic waves leading to beam deflection through significant deviation angles are of sufficiently high frequency that they are typically strongly attenuated over distances of a several cm. This limits the effective aperture and hence the angular resolution that can be achieved.

We proposed to circumvent these problems by applying nonlinear optical techniques to AO beam steering. Specifically, we noted that the photoelastic effect which allows sound waves to deflect light in an AO beam deflector implies the existence of an electrostrictive effect in the same material. This electrostrictive effect implies that the electric field of light passing through the medium will generate a sound wave in the medium. Furthermore, we showed that in an AO device, this optically generated sound wave should be formed in phase with the original sound wave causing the beam deflection in the medium. Thus this nonlinear optical phenomenon serves to amplify the acoustic waves already present in an AO device. The results of this effect are twofold. First, optical power is now converted to acoustic power in the device reducing the power requirements on the acoustic signal introduced into the material by conventional transducers. Second, the amplification of the acoustic wave occurs progressively as the wave propagates through the material. Thus the nonlinear optical process provides an acoustic gain process that counteracts the high frequency loss seen in standard AO systems. Thus an AO beam deflector utilizing this nonlinear optical enhancement technique should be able to support an acoustic wave over a substantially broader effective aperture and hence provide substantially improved angular resolution. The primary goal of this contract was the demonstration of this nonlinear optical enhancement technique of AO beam deflection and to show the feasibility of this approach for high power, high accuracy beam steering.

Results

The work performed under this program consisted of a series of innovations in the theory of nonlinear optical effects in acousto-optic media, and experiments designed to demonstrate effective nonlinear optical enhancement of AO beam deflection. This demonstration was carried out in three stages which are documented in detail in the three reprinted publications which follow this summary. In brief, these stages corresponded to:

1. An initial demonstration of the nonlinear optical enhancement effect in an off-the-shelf AO beam deflector.

2. A demonstration of an improved system geometry yielding an order of magnitude greater enhancement in the same standard device.

and

3. A demonstration of a prototype AO device specially designed to allow for optimum nonlinear optical enhancement. This last device allowed us improve the diffraction efficiency of the AO device by two orders of magnitude using our nonlinear optical technique.

These experimental results conclusively show that nonlinear optical enhancement of AO diffraction permits high diffraction efficiencies to be obtained with low acoustic drive powers. Furthermore at such high levels of gain, the acoustic attenuation is sufficiently compensated that substantial increases in the effective aperture have been obtained. These results suggest that the demonstration level systems examined under this program may be successfully scaled up into large aperture systems capable of directing MW, and GW level laser pulses with an accuracy on the order of 10 μrad and response times of tens of μsec.

The results of the effort are summarized in the form of three refereed papers, detailing the results of our modeling and experiments. A section included at the end of this report examines system application of the concepts studied in this program, for Rapid Optical Beam Steering (ROBS) efforts of interest to BMDO (SDI).

Enhanced acousto-optic diffraction in electrostrictive media

Frederick Vachss, Ian McMichael, Monte Khoshnevisan, and Pochi Yeh

Rockwell International Science Center, Thousand Oaks, California 91360

Received June 22, 1989; accepted November 13, 1989

We examine the phenomenon of light-induced enhancement of the acoustic waves traveling in electrostrictive materials. In particular, we consider the case of an acousto-optic Bragg cell illuminated by an intense optical beam and show that the diffraction efficiency of the device may exhibit an intensity dependence that is due to the electrostrictive nonlinearity of the acousto-optic medium. We describe experiments in which high-energy pulsed laser sources are used to show a 20% enhancement in the diffraction efficiency observed in a TeO_2 acousto-optic modulator.

1. INTRODUCTION

Acousto-optic modulators used as Bragg cells provide an efficient, readily controllable means of deflecting and modulating optical beams and are used in a wide variety of optical device applications. In their simplest form, acousto-optic (AO) devices act as holographic phase gratings and deflect incident optical beams by diffraction from refractive-index variations within the AO medium. Index gratings in AO media, however, unlike those in standard optically sensitive holographic recording media, are induced by the presence of a traveling acoustic wave launched into the medium and coupled to the refractive index through the linear photoelastic effect. The strength of the grating (i.e., the magnitude of the refractive-index variation within the material) is thus directly dependent on the acoustic intensity transferred to the medium. Since the diffraction efficiency of a holographic phase grating is determined by the optical thickness of the grating as well as by the grating strength, the total acoustic power required to obtain a given diffraction efficiency for a given device aperture and optical thickness provides a fundamental figure of merit describing the usefulness of AO materials in diffractive applications.[1] As the required acoustic power increases with the useful aperture of the device, this power requirement may become a severe device limitation in beam-steering applications requiring fine angular resolution and hence commensurately large apertures.

The description above, however, assumes that the strain wave within the material is entirely mechanically induced and ignores the influence of the optical fields present on the acoustic field within the medium. The electrostrictive and electrocaloric effects underlying various stimulated scattering processes are well known[2] and permit the optical modification of local acoustic waves. In particular, the electrostrictive effect provides a direct feedback from the optical electric fields to the material strain field and has been used by several investigators[3,4] to demonstrate the optical generation and amplification of acoustic waves.

It has been shown by Yeh and Khoshnevisan[5] that the presence of such an electrostrictive nonlinearity in an AO device should allow for enhancement of the acoustic grating strength through the interaction of the incident and diffracted optical fields within the material. This analysis, in fact, indicated that for sufficiently high incident optical intensities the electrostrictively induced grating would grow sufficiently large that the positive feedback between the optical and acoustic fields would drive the AO device to high diffraction efficiencies—even when the initial purely acoustically induced efficiency was quite low. Such a positive feedback effect could thus allow for the efficient steering of high-power optical beams at acoustic power levels well below those calculated by using the standard AO figure of merit for diffraction described above.

The analysis of Yeh and Khoshnevisan from which these results were derived, however, considered the case of an AO device used to diffract an intense cw plane wave of infinite transverse spatial extent. We show in this paper that this analysis must be modified considerably to describe the more realistic case of finite-sized beams of limited duration, such as those that result when high-intensity pulsed sources are focused into an AO cell to obtain high optical power densities. We then show, as a result of this analysis, that the nonlinear AO enhancement described by Yeh and Khoshnevisan occurs with spatiotemporally finite sources as well but at substantially higher optical power levels than those calculated in the earlier cw plane-wave analysis. In particular, this analysis results in an explicit expression for the optical power thresholds required for enhanced diffraction to occur. The theoretical threshold behavior that we predict is then verified by showing an intensity-dependent acousto-optic diffraction efficiency in a TeO_2 Bragg cell under high-power pulsed illumination.

2. THEORETICAL BACKGROUND

A. Basic Formulation

We shall consider the case of an AO device illuminated by an optical beam of finite size and duration as depicted in Fig. 1. Here we assume that a transducer located at the $x = 0$ plane introduces an acoustic wave into the medium traveling in the positive $\mathbf{x}$ direction, yielding a density modulation of the form

$$\Delta\rho_{ac}(\mathbf{r}, t) = \rho_1 \exp[i\Omega(x/v - t) - x/L_{ac}] + \text{c.c.}, \qquad (1)$$

where ρ_1 is the strength of the acoustic grating; Ω is the excitation frequency, which we assume is near the device's acoustic resonance; v is the acoustic velocity; and L_{ac} is the

0740-3224/90/050859-09$02.00

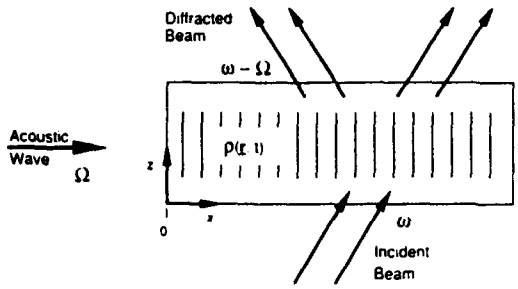

Fig. 1. Basic AO Bragg deflector geometry, showing the frequency shift of the diffracted beam.

acoustic attenuation length of the medium. Since this acoustic grating results in a proportional refractive-index variation through the medium's photoelastic response, the incident optical field will diffract from this grating to generate a second beam within the medium. This allows us to write the total optical electric field amplitude in the device as

$$E(\mathbf{r}, t) = R(\mathbf{r}, t)\exp[i(\mathbf{k}_1 \cdot \mathbf{r} - \omega_1 t)] + S(\mathbf{r}, t)\exp[i(\mathbf{k}_2 \cdot \mathbf{r} - \omega_2 t)] + \text{c.c.}, \quad (2)$$

where R and S are the amplitude envelopes of the incident and diffracted beams, respectively, and $\mathbf{k}_i$ and ω_i $(i = 1, 2)$ are the nominal propagation vectors and center frequencies of the two beams. By expressing the fields in this form we implicitly assume that the envelope functions are of sufficiently narrow spatial and temporal bandwidth that this modulated plane-wave expression remains valid. We finally assume that the incident beam is tuned to the Bragg angle of the AO cell so as to maximize the diffracted output. In this case, assuming that the acoustic damping is small, we obtain the conservation relations

$$\omega_2 = \omega_1 \pm \Omega, \qquad \mathbf{k}_2 = \mathbf{k}_1 \pm (\Omega/v)\hat{x}, \quad (3)$$

where $\hat{x}$ is a unit vector parallel to the acoustic grating vector. These imply the usual AO result that the diffracted wave is either frequency upshifted or downshifted from the incident wave by the acoustic frequency, depending on the orientation of the incident wave.[1] The description presented above, though correct to leading order for low-power optical beams, ignores the effects of the optical fields on the acoustic grating that we wish to address. To obtain the equations describing this optical feedback, we shall essentially follow the standard derivation of Kaiser and Maier[2] describing stimulated scattering processes.

It is well known that a linear relationship between the strain and the refractive index in any medium through some photoelastic coefficient implies that the electrostatic energy density of the medium must be similarly coupled to the strain. This in turn implies the existence of an electrostrictive force on any volume element of the medium with magnitude proportional to that of the photoelastic coefficient. Specifically, if we write

$$\Delta\epsilon(\mathbf{r}, t) = \gamma S(\mathbf{r}, t) = \gamma\Delta\rho(\mathbf{r}, t)/\rho_0, \quad (4)$$

relating perturbations in the dielectric constant ϵ to the strain S (or, equivalently, to the density perturbation $\Delta\rho$ divided by the bulk average density ρ_0) through the coupling coefficient γ, we must similarly write

$$\mathbf{F}(\mathbf{r}, t) = \frac{1}{8\pi}\gamma\nabla(E^2), \quad (5)$$

where $\mathbf{F}$ is the local electrostrictive force per unit volume and E is the local electric field amplitude. While in principle the electrostrictive coupling constant γ defined in Eq. (4) above is a fourth-rank tensor relating the second-rank strain and dielectric tensors, for simplicity we shall restrict our remaining discussion to scalar interactions and shall thus use the expressions given above.

Equation (5) in particular provides an inhomogeneous driving term, allowing us to write the combined Navier–Stokes and continuity equations for the density perturbation in the medium in the form

$$-d^2(\Delta\rho)/dt^2 + v^2\nabla^2(\Delta\rho) + (2v^3/\Omega^2 L_{ac})\frac{d}{dt}\nabla^2(\Delta\rho) = \frac{1}{8\pi}\gamma\nabla^2(E^2), \quad (6)$$

where we recall that v, Ω, and L_{ac} are the acoustic velocity, excitation frequency, and attenuation length, respectively. In deriving this equation we have implicitly ignored thermal effects, as is reasonable in typical weakly absorbing AO media. In the typical situation in which the acoustic attenuation length far exceeds the acoustic period, we observe that the injected density wave amplitude $\Delta\rho_{ac}$ given in Eq. (1) is a solution of the homogeneous form of Eq. (6) for all values of the grating strength ρ_1. The full solution for the density wave in the medium can thus be expressed as

$$\Delta\rho(\mathbf{r}, t) = \Delta\rho_{ac}(\mathbf{r}, t) + \Delta\rho_{opt}(\mathbf{r}, t), \quad (7)$$

where $\Delta\rho_{ac}$ is the mechanically generated component of the acoustic wave given in Eq. (1) and the optically generated component $\Delta\rho_{opt}$ satisfies Eq. (6) with $\Delta\rho_{opt}(\mathbf{r}, t) = 0$ when the optical field strength is zero. We must now obtain the optically generated acoustic field amplitude as a function of the two optical beam amplitudes.

When substituting Eq. (2) into the right-hand side of Eq. (6) we find 16 possible terms in the squared amplitude. Of these, however, most will oscillate at frequencies far from the acoustic resonance and give rise to minimal acoustic excitation. We thus include only those terms oscillating near resonance to obtain

$$-d^2(\Delta\rho_{opt})/dt^2 + v^2\nabla^2(\Delta\rho_{opt}) + (2v^3/\Omega^2 L_{ac})\frac{d}{dt}\nabla^2(\Delta\rho_{opt}) \approx \frac{1}{4\pi}\gamma\nabla^2[R^*(\mathbf{r}, t)S(\mathbf{r}, t)\exp[\pm i\Omega(x/v - t)] + \text{c.c.}], \quad (8)$$

where the sign of the exponential argument is determined by the sign of the frequency difference between the incident and diffracted optical beams. We recognize Eq. (8) as a damped driven wave equation whose solution is obtained by using Fourier-transform methods in Appendix A. The result of this appended derivation is

$$\Delta\rho_{opt}(\mathbf{r}, t) = \pm[\gamma\Omega/(8\pi i v^2)]\exp[\pm i\Omega(x/v - t)]\int_0^\infty [\exp(\pm 2i\Omega s) \times f(\mathbf{r} + vs\hat{x}, t - s) - f(\mathbf{r} - vs\hat{x}, t - s)]\exp(-vs/L_{ac})ds + \text{c.c.}, \quad (9)$$

where $f(\mathbf{r}, t) \equiv R^*(\mathbf{r}, t)S(\mathbf{r}, t)$ is the amplitude of the optical interference term driving the acoustic response and we assume that the incident beam amplitude $R(\mathbf{r}, t)$ is turned on at time $t = 0$.

B. Preliminary Results

The above result shows that the optically induced component of the acoustic wave $\Delta\rho_{opt}$ consists of a slowly varying amplitude modulation superposed upon a plane-wave carrier term oscillating at frequency Ω and traveling with velocity v and hence tracking the mechanically induced wave component $\Delta\rho_{ac}$. Thus $\Delta\rho_{opt}$ will provide a coherent contribution to the refractive-index grating initially generated by $\Delta\rho_{ac}$, and we may expect significant modification in the diffraction efficiency of the overall grating when the amplitude of $\Delta\rho_{opt}$ approaches that of $\Delta\rho_{ac}$. Our effective optical power threshold for the nonlinear enhancement of AO diffraction will thus be roughly that required to obtain $|\Delta\rho_{opt}| \approx |\Delta\rho_{ac}|$. In Subsection 2.C we shall formalize this heuristic result by including the optically generated acoustic wave in the coupled equations for AO diffraction.

Before proceeding to this formal analysis, however, it is instructive to compare the result given in Eq. (9) above with its plane-wave steady-state limiting form. When the incident beam (and hence the diffracted beam) is a cw plane wave, the beam envelope functions $R(\mathbf{r}, t)$ and $S(\mathbf{r}, t)$ are spatiotemporal constants, and Eq. (9) may be simplified to obtain

$$\Delta\rho_{opt}(\mathbf{r}, t) \approx \pm[i\gamma\Omega L_{ac}/(8\pi v^3)]\exp[\pm i\Omega(x/v - t)]R^*S + \text{c.c.}, \tag{10}$$

where we have assumed that $\Omega L_{ac}/v \gg 1$ (i.e., that many acoustic periods are contained within the acoustic attenuation length) in obtaining this result. We thus see that, in this plane-wave limit, the optically induced density perturbation is directly proportional to the local intensity interference pattern, $I(\mathbf{r}, t) \equiv c\langle E^2\rangle/4\pi$ (where $\langle \ldots \rangle$ here denotes a time average over several optical cycles). Thus, given the linear photoelastic coupling between the density and the refractive index, $n(\mathbf{r}, t)$, we obtain a Kerr-like optical nonlinearity [i.e., $n(\mathbf{r}, t) = n_0 + n_2 I(\mathbf{r}, t)$], as assumed in the description by Yeh and Khoshnevisan of this limiting case.

In the more general case described by Eq. (9), however, this proportional behavior breaks down, and the density perturbation depends instead on traveling-wave integrals of the optical intensity, i.e., temporal integrals of the optical intensity distribution evaluated at a point moving with a given velocity so that both the space and the time coordinates vary simultaneously. Specifically, the density expressed in Eq. (9) is proportional to the difference of two such integrals, a *forward* solution traveling with the acoustic wave at the acoustic velocity and a *backward* solution traveling in the opposite direction at the same speed. We note that the backward solution contains an additional phase factor of $\exp(\pm 2i\Omega s)$ in the integrand not found in the forward solution. For slowly varying optical amplitude envelopes this implies that, while initially the two solutions will tend to cancel each other out, after a few acoustic periods (i.e., for $\Omega t \gg 1$) the oscillations introduced by the phase term in the backward solution will average this solution to near zero and allow the forward solution to dominate. This in turn implies that optical pulses of duration less than the acoustic period $\tau_{ac} \equiv 2\pi/\Omega$ will not efficiently excite acoustic waves within the medium. We thus restrict our remaining analysis to the more useful limit of incident intensity pulses with durations long compared with τ_{ac}, in which case the density wave reduces to only the forward solution:

$$\Delta\rho_{opt}(\mathbf{r}, t) = \pm[i\gamma\Omega/(8\pi v^2)]\exp[\pm i\Omega(x/v - t)] \times \int_0^t \exp(-vs/L_{ac})f(\mathbf{r} - vs\hat{\mathbf{x}}, t - s)\,ds + \text{c.c.} \qquad (\text{for } \Omega t \gg 1). \tag{11}$$

Another implication of the traveling-wave form of the induced density wave given in Eq. (11) is the nonlocal nature of the acoustic response. Assuming that the driving intensity pattern $f(\mathbf{r}, t)$ is spatially localized within some spot diameter D (as would be the case for a focused beam), we see that, while the integral expression is initially localized as well, for times greater than the spot-size transit time D/v the optically induced acoustic wave propagates out of the region of illumination. Indeed, if we model the optical interference term (albeit somewhat coarsely) by assuming that

$$f(r, t) = R^*(y, z)S(y, z), \quad 0 < x < D, \quad t > 0$$
$$= 0, \quad \text{otherwise} \tag{12}$$

(i.e. the driving term is uniform in the grating direction in the illuminated region), we may explicitly evaluate Eq. (11) to obtain

$$\Delta\rho_{opt}(\mathbf{r}, t) = \pm i\gamma\Omega L_{ac}/(8\pi v^3)\exp[\pm i\Omega(x/v - t)] \times R^*S \times [1 - \exp(-x/L_{ac})] \tag{13}$$

for $0 < x < D$ and $t > D/v$. We recognize this as exactly the steady-state plane-wave solution for the density given in formula (10) multiplied by a factor of $[1 - \exp(-x/L_{ac})]$. This multiplicative factor has two main implications. First, the density wave will be nonuniform and will grow in the direction of acoustic propagation. More importantly, the magnitude of this exponential factor is always bounded by D/L_{ac} for x in the illuminated region. Hence for small spot sizes the acoustic wave amplitude is reduced by a factor of the order of the spot size over the attenuation length from the plane-wave value. Although it was derived for a specific intensity distribution, this last result remains valid for any spatially localized distribution and is the fundamental reason for the discrepancy between the optical power thresholds for diffraction efficiency enhancement calculated by Yeh and Khoshnevisan in the plane-wave limit and those that we shall determine in the following subsection for more-general beam types.

C. Coupled-Wave Analysis

To determine the effective diffraction efficiency of the AO device as a function of the incident optical intensity, we must obtain equations describing the propagation and coupling of the optical beams within the medium. Following the standard holographic coupled-wave treatment of Kogelnik,[6] we start with the scalar wave equation for the optical field within the medium:

$$\nabla^2 E(\mathbf{r}, t) - \frac{\epsilon(\mathbf{r}, t)}{c^2}\frac{d^2E(\mathbf{r}, t)}{dt^2} = 0, \tag{14}$$

where we have assumed for simplicity that the medium is

optically isotropic. Substituting Eqs. (2) and (4) into Eq. (14) and assuming that the spatiotemporal beam envelopes vary slowly on the scales of the optical spatial and temporal frequencies, we obtain

$$2i\mathbf{k}_1\cdot\nabla R(\mathbf{r},t)\exp[i(\mathbf{k}_1\cdot\mathbf{r}-\omega_1 t)]+2i\mathbf{k}_2\cdot\nabla S(\mathbf{r},t)$$
$$\times\exp[i(\mathbf{k}_2\cdot\mathbf{r}-\omega_2 t)]=-\frac{\gamma\Delta\rho(\mathbf{r},t)}{\rho_0 c^2}[\omega_1^2 R(\mathbf{r},t)$$
$$\times\exp[i(\mathbf{k}_1\cdot\mathbf{r}-\omega_1 t)]+\omega_2^2 S(\mathbf{r},t)\exp[i(\mathbf{k}_2\cdot\mathbf{r}-\omega_2 t)]]. \quad (15)$$

Note that in obtaining this equation we retain first-order spatial derivatives of the beam envelope functions while discarding terms containing first-order temporal derivatives of these quantities, which are generally much smaller in magnitude (of the order of v/c, the ratio between the acoustic and optical velocities). Now, using Eq. (7) and the specific forms for the two components of $\Delta\rho$ in Eqs. (1) and (11), we may collect terms with similar exponential factors and use stationary phase arguments to separate Eq. (15) into the following pair of coupled equations for the incident and diffracted beam envelope functions:

$$\frac{dS}{dz}=\left\{-i\kappa\exp(-x/L_{ac})\pm g\int_0^t\exp(-vs/L_{ac})\right.$$
$$\left.\times R^*(\mathbf{r}-v s\hat{\mathbf{x}},t-s)S(\mathbf{r}-v s\hat{\mathbf{x}},t-s)ds\right\}R \quad (16a)$$

and

$$\frac{dR}{dz}=-\left\{i\kappa\exp(-x/L_{ac})\pm g\int_0^t\exp(-vs/L_{ac})\right.$$
$$\left.\times S^*(\mathbf{r}-v s\hat{\mathbf{x}},t-s)R(\mathbf{r}-v s\hat{\mathbf{x}},t-s)ds\right\}S, \quad (16b)$$

where

$$\kappa\equiv\gamma\rho_1\omega/(2\rho_0 nc) \quad (17a)$$

is the Bragg coupling coefficient of the unenhanced AO grating and

$$g\equiv\gamma^2\Omega\omega/(16\pi v^2\rho_0 nc)=M_3\Omega/(32\lambda) \quad (17b)$$

is a parameter describing the magnitude of the nonlinear coupling enhancement, with n defined as the medium's average refractive index, λ as the free-space optical wavelength, and M_3 as one of the standard[1] figures of merit characterizing the AO properties of the medium. Note that in obtaining Eqs. (16a) and (16b) we have used the fact that Ω (typically $\sim 10^8$ Hz) is much less than the optical frequency to write $\omega_1\approx\omega_2\equiv\omega$ and $k_1\approx k_2\equiv k=\omega n/c$, and the assumption that $\Omega/v\ll k$ (i.e., that the beam deflection angle is small) to write $\mathbf{k}_1\approx\mathbf{k}_2=k\mathbf{z}$.

The amplitude envelopes of the interacting beams within the material may thus be obtained by solving the pair of coupled first-order nonlinear integrodifferential equations given in Eqs. (16a) and (16b). While the analytic solution of this coupled system is achievable, the required derivation is rather time consuming and is not, in fact, necessary for the optical power threshold for enhanced AO diffraction to be calculated. For simplicity we thus shall restrict our derivation to the regime of relatively low diffraction efficiency in this paper and defer the full solution of the coupled system above to a later publication describing the saturated nonlinear regime.

This restriction allows us to assume that κ is sufficiently small that $R(\mathbf{r},t)$ is effectively independent of z within the medium. Making this assumption reduces the problem to that of solving the single equation [Eq. (16a)] for $S(\mathbf{r},t)$. This solution may be obtained by using an analytic technique similar to that presented by Kroll[7] in his treatment of the related problem of optically induced acoustic instabilities. We proceed by expressing the solution for the diffracted beam amplitude as a power series in the parameter g/κ of the form

$$S(\mathbf{r},t)=\sum_{n=0}^{\infty}S_n(\mathbf{r},t)(g/\kappa)^n. \quad (18)$$

Substituting this form into Eq. (16a) and using the assumption of weak depletion to write $R(x,y,z,t)\approx R(x,y,0,t)\equiv R_0(x,y,t)$, we obtain

$$dS_0/dz=-i\kappa\exp(-x/L_{ac})R_0(x,y,t) \quad (19a)$$

and, for $n>0$,

$$dS_n/dz=\pm\kappa R_0(x,y,t)\int_0^t\exp(-vs/L_{ac})$$
$$\times R_0^*(x-vs,y,t-s)S_{n-1}(x-vs,y,t-s)ds. \quad (19b)$$

Solving Eq. (19a) and then iterating the solution of Eq. (19b), we obtain the general result:

$$S_n(x,y,z,t)=-iR_0(x,y,t)\exp(-x/L_{ac})$$
$$\times\frac{\left[\pm\int_0^t|R_0(x-vs,y,t-s)|^2ds\right]^n}{n!}\frac{(\kappa z)^{n+1}}{(n+1)!}. \quad (20)$$

Substituting Eq. (20) into Eq. (18), we then have an explicit power series representation of $S(\mathbf{r},t)$ that we may sum directly to obtain[8]

$$S(x,y,z,t)=-i\kappa zR_0(x,y,t)\exp(-x/L_{ac})$$
$$\times H\left(\pm gz\left[\int_0^t|R_0(x-vs,y,t-s)|^2ds\right]\right), \quad (21a)$$

where the function H is defined as

$$H(u)\equiv\begin{cases}I_1(2u^{1/2})/u^{1/2}, & u>0\\ J_1(2|u|^{1/2})/|u|^{1/2}, & u<0\end{cases} \quad (21b)$$

and J_1 and I_1 are the ordinary and modified Bessel functions of the first kind, respectively. Since the argument of H in Eq. (21a) becomes small for weak optical feedback into the acoustic grating (i.e., when g or $|R|^2$ is sufficiently small that nonlinear effects are negligible) and since $H(u)\to 1$ as $u\to 0$, we see that Eq. (21a) may be rewritten as

$$S(\mathbf{r},t)=S_0(\mathbf{r},t)H\left(\pm gz\left[\int_0^t|R_0(x-vs,y,t-s)|^2ds\right]\right), \quad (22a)$$

where

$$S_0\equiv-i\kappa zR_0(x,y,t)\exp(-x/L_{ac}) \quad (22b)$$

is the diffracted beam amplitude in the absence of optically

induced nonlinear effects. H is thus a factor describing the gain or loss factor by which this amplitude is multiplied owing to the optical feedback. Similarly, the diffraction efficiency of the device may be written as

$$\eta = |S(x, y, L, t)|^2/|R_0(x, y, t)|^2$$
$$= \eta_0\left\{H\left(\pm gL\left[\int_0^t |R_0(x - vs, y, t - s)|^2 ds\right]\right)\right\}^2, \quad (23)$$

where L is the depth of the medium and $\eta_0 \equiv |S_0|^2/|R_0|^2$ is the unenhanced diffraction efficiency. The intensity-dependent diffraction enhancement that we hope to describe is thus completely characterized by the functional behavior of H in Eqs. (22a) and (23) above.

This behavior is illustrated in Fig. 2, where $H(u)$ is plotted versus u over the interval $-5 < u < 5$. We observe from this plot that, while $H(u)$ is linear with a slope of 0.5 in the region of $u \approx 0$, $H(u)$ decays rapidly to zero as $u \to -\infty$ but grows with increasing rapidity for increasing $u > 0$. This is a reflection of the fact that, while $J_1(u)$ asymptotically exhibits a decaying oscillatory behavior for large u, $I_1(u)$ tends to grow exponentially without bound as u is increased.

This behavior has a variety of physical implications in the diffraction process. First we recall that the sign of the argument of H in Eq. (22a) is determined by the sign of the frequency shift of the diffracted beam with respect to that of the incident beam, with negative frequency shifts yielding a positive argument and vice versa. This implies that when the optical field loses energy to the acoustic field in the diffraction process, this lost energy is manifested as an amplified acoustic grating resulting in increased diffraction, while the opposite process of grating deenhancement must occur when energy is removed from the acoustic grating. Physically these inverse processes may be thought of as the creation or annihilation of phonons from the acoustic field required by energy conservation whenever an incident photon is diffracted from the grating with an associated frequency shift. Thus, for sufficiently high intensities that the magnitude of the argument of H in Eq. (22a) approaches unity, we should see a significant enhancement or reduction in the diffraction efficiency of the AO device—with the sign of the modification in the efficiency controlled by the direction of the incident beam with respect to that of the propagating acoustic wave in the medium.

Furthermore, we note that, while the response is roughly linear in the argument of H for operation near the enhancement threshold, the unbounded growth of $H(u)$ for $u > 0$ implies that, for any initial diffraction efficiency, sufficiently high input intensity will drive the device to ever higher diffraction efficiencies until substantial depletion of the incident optical field results. More importantly, the exponential nature of this growth implies that the incident intensity required for this high-diffraction-efficiency result to occur is only weakly (roughly logarithmically) dependent on the initial diffraction efficiency of the device. Thus, even for rather low initial efficiency levels, there will be an intensity threshold above which the AO device will be driven into the high-efficiency depleted-pump regime. This qualitatively duplicates the earlier plane-wave result of Yeh and Khoshnevisan, showing the potential of the optical feedback effect to yield high diffraction efficiency at low acoustic power levels.

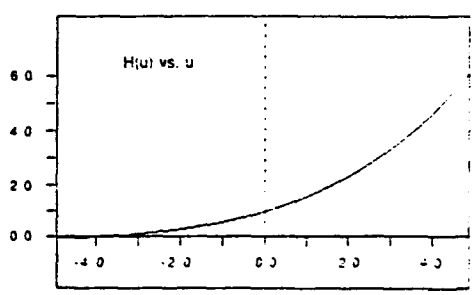

Fig. 2. Amplitude response function $H(u)$ plotted for $-5 < u < 5$. Note the nearly exponential behavior for both positive and negative arguments.

D. Calculation of Enhancement Threshold

While the analysis used to obtain these results fails to describe the diffraction process accurately once substantial depletion of the incident beam has occurred, the implication that this depleted-pump regime is achieved remains valid, and the rate at which this operating regime is approached is still well described by Eq. (22a). As the final result of this section we shall thus use Eq. (22a) to derive the optical power threshold for enhanced AO diffraction. Using the arguments of the previous two paragraphs, we rather arbitrarily define for this threshold the requirement that the argument of H in Eq. (22a) be of the order of unity and thus obtain

$$gL\left[\int_0^t |R_0(x - vs, y, t - s)|^2 ds\right] = 1 \quad (24)$$

as our threshold requirement. It is interesting to note that, since Eq. (23) expresses the diffraction efficiency as the unenhanced value η_0 multiplied by the gain function H, our threshold condition depends solely on the argument of this gain function and is thus independent of η_0 and the coupling coefficient κ. We now assume for convenience that the incident intensity distribution $I_0(x, y, t) \equiv c|R_0(x, y, t)|^2/2\pi$ can be expressed in the separable form

$$I_0(x, y, t) = F_x(x)F_y(y)I(t), \quad (25)$$

where $I(t)$ is the instantaneous maximum intensity in the illuminated region and F_x and F_y are spatially localized functions normalized to a maximum value of unity with effective widths of D_x and D_y, respectively, satisfying $\int_{-\infty}^{\infty} F_x(x)dx = D_x$ and $\int_{-\infty}^{\infty} F_y(y)dy = D_y$.

Given this decomposition, we find that, while the exact value of the integral in Eq. (24) depends on the functional forms of these pulse shape functions, the integral in general is bounded by

$$\int_0^t |R_0(x - vs, y, t - s)|^2 ds \le \frac{2\pi}{c} I_{max} \min(t, D_x/v), \quad (26)$$

where I_{max} is the maximum instantaneous intensity reached during the optical pulse and $\min(t, D_x/v)$ denotes the lesser of these two times. Replacing the integral by its upper bound and substituting into Eq. (22a), we thus obtain

$$I_{\text{threshold}} = \left[\frac{2\pi}{c} gL \min(t, D_x/v)\right]^{-1} \tag{27}$$

as our intensity threshold for enhanced diffraction. Since the average intensity within the illuminated spot is, in general, less than $I_{\max}$ and the transverse spot width is typically less than D_x (other than through the center of the spot), we expect that our true threshold intensity will be somewhat higher than that given in this expression. Nonetheless this result provides a reasonable estimate of the true threshold value. Examining Eq. (27), we note that, for pulse durations less than the spot-size transit time, the intensity threshold is reduced simply by lengthening the pulse and keeping the total pulse energy the same. Similarly for longer pulse durations, the threshold intensity may be reduced while keeping the total energy constant by increasing the transverse spot width D_x. We note, however, that such increases in spot diameter become ineffective in enhancing the acoustic diffraction for $D_x > L_{ac}$ owing to the decaying exponential behavior of $S_0(\mathbf{r}, t)$ shown in Eq. (22b).

In particular, in the regime of pulse durations long relative to the spot-size transit time, we may use the definition of g in Eq. (17b) to rewrite Eq. (27) as

$$I_{\text{threshold}} = [M_2(nLD_x\Omega\omega/32c^2)]^{-1} \tag{28}$$

in terms of the standard AO efficiency figure of merit M_2,[1] which relates the strength of refractive-index modulation to the acoustic intensity. This term is multiplied by a dimensionless factor determined by the device thickness, spot size, and acoustic and optical driving frequencies. From the results of Eqs. (27) and (28) we see that the enhancement intensity threshold intrinsically depends on the duration and size of the incident light pulse as well as on material properties through M_2. This is perhaps the most fundamental difference between our result and that obtained from the earlier plane-wave analysis of Yeh and Khoshnevisan, showing a threshold strictly dependent on the properties of the AO device.

3. EXPERIMENTAL CONFIRMATION

The analysis given in the preceding section indicates that enhanced AO diffraction can most easily be achieved in materials with high values of the appropriate AO figure of merit. The experiments that we shall describe were thus performed with a TeO_2 slow-shear wave AO modulator—in which the M_2 figure of merit is almost 1000 times that of fused silica.[1] Our analysis also indicates that intensity thresholds will be minimized by using optical pulses with durations well exceeding the inverse acoustic frequency and at least as long as the spot-size transit time. For this reason we elected to use the Chroma laser facility at KMS Fusion, a relatively high-energy, long-pulse-duration laser source, to confirm the enhancement effect.

The Chroma laser consists of a Nd:YLF oscillator/Nd:glass amplifier system and is capable of producing pulses of greater than 50-J total energy and 100-μsec duration at an operating wavelength of 1.05 μm. While such high energy levels are not necessary for threshold enhancement to be achieved (and, indeed, would damage the AO device), this capability allows for precise control of the temporal pulse shape at lower pulse energies by using a novel system developed at KMS.[9] This control is achieved by monitoring the laser output during the pulse with a fast photodetector, electronically comparing the detector output with the desired pulse shape function, and using the amplified difference between these two signals to modulate the oscillator output and close the feedback loop.

We now note that Eqs. (23), (25), and (27) imply that near threshold the diffraction efficiency of the device may be written as

$$\begin{aligned}\eta(x, y, t) &= \eta_0\left\{1 \pm gL\left[\int_0^t |R_0(x - vs, y, t - s)|^2 ds\right]\right\} \\ &\approx \eta_0\left[1 \pm gL \frac{2\pi}{c} \langle I(t)\rangle F_y(y)/v \int_{-\infty}^{x} F_x(x')dx'\right] \\ &\qquad \text{for } t \gg D_x/v \\ &= \eta_0\left[1 \pm F_y(y)/D_x \int_{-\infty}^{x} F_x(x')dx' \langle I(t)\rangle / I_{\text{threshold}}\right],\end{aligned} \tag{29}$$

where $\langle I(t)\rangle$ is the peak incident intensity defined in Eq. (25), averaged over a time interval of $\Delta t \approx D_x/v$ before t. While this expression describes the profile of the diffraction efficiency across the illuminated spot, the quantity usually observed experimentally is the spatial average diffraction efficiency, defined by

$$\begin{aligned}\eta_{\text{av}}(t) &\equiv \frac{\iint_{-\infty}^{\infty} |S(x, y, t)|^2 dx dy}{\iint_{-\infty}^{\infty} |R_0(x, y, t)|^2 dx dy} \\ &= \frac{\iint_{-\infty}^{\infty} \eta(x, y, t)|R_0(x, y, t)|^2 dx dy}{\iint_{-\infty}^{\infty} |R_0(x, y, t)|^2 dx dy} \\ &= \eta_0\left\{1 \pm \int_{-\infty}^{\infty} [F_y(y)]^2 dy \int_{-\infty}^{\infty} F_x(x)dx \int_{-\infty}^{x} F_x(x')dx' \right. \\ &\qquad \left. \times \langle I(t)\rangle / [I_{\text{threshold}}(D_x)^2 D_y]\right\} \\ &= \eta_0\left(1 \pm \left\{\int_{-\infty}^{\infty} [F_y(y)]^2 dy/D_y\right\} \langle I(t)\rangle/(2I_{\text{threshold}})\right),\end{aligned} \tag{30}$$

where we have used expression (29), the decomposition of $|R_0|^2$ in Eq. (25), and the normalization condition for $F_x(x)$ given in Subsection 2.D in obtaining this result. The quantity in the second set of braces in this expression is a dimensionless factor whose value depends on the degree of uniformity of $F_y(y)$ but is typically near unity—with a value of 1.0 when F_y is a uniform rect function and a value of $1/\sqrt{2}$ when F_y is a Gaussian.

For pulse durations long compared with the spot-size transit time, we thus expect to see a linear dependence of the time-resolved diffraction efficiency $\eta_{\text{av}}(t)$ on the incident intensity $\langle I(t)\rangle$. Furthermore, equal and opposite modifications of the diffraction efficiency should result for the two configurations corresponding to opposite signs of the frequency shift of the diffracted beam. Hence, by performing a time-resolved measurement of the diffraction efficiency, we not only obtain a complete time-multiplexed measurement of the diffraction efficiency of the device as a function

of the incident intensity with each pulse but also, by comparing these results for the two orientations, obtain a sensitive probe of the optically induced modification of the diffraction efficiency.

This input pulse shaping/time-resolved measurement technique was implemented with the setup depicted in Fig. 3. Here the electronic feedback system described earlier in this section is used to generate a triangular input pulse 20 μsec in duration, as shown, with a 10-μsec linear rise followed by a symmetric 10-μsec linear decay. This beam is then focused and collimated, resulting in a spot roughly 1 mm in diameter (FWHM) incident upon the surface of the TeO_2 cell. We note that since the acoustic velocity in this material is 6.2×10^2 m/sec, the spot-size transit time is 1.6 μsec and is thus substantially less than the pulse duration, satisfying the criterion in expression (29). The 1-cm-deep AO cell was driven at a frequency of 80 MHz with sufficient acoustic power to result in 20% diffraction efficiency at low incident optical intensities. Using Eq. (28), we find that for this set of experimental parameters our calculated intensity threshold for nonlinear diffraction enhancement is $I_{\text{threshold}} \approx 19$ MW/cm^2.

Following the description in the preceding paragraph, the cell was oriented at the Bragg angle for either of the two diffraction configurations and the incident and diffracted intensity directed into photodiodes. These diodes were then monitored in real time, sampled by an analog-to-digital converter at 100-nsec intervals, and the results then stored, yielding a 200-point data set describing the incident and diffracted intensities as a function of time over each 20-μsec optical pulse. By using the incident intensity data set and the point-by-point ratio of the two sets, we thus obtained a time-resolved representation of $I(t)$ and $\eta_{av}(t)$ by which the threshold result of expression (29) could be checked. Such measurements were conducted repeatedly at increasingly high pulse energies until permanent optical damage of the AO cell resulted.

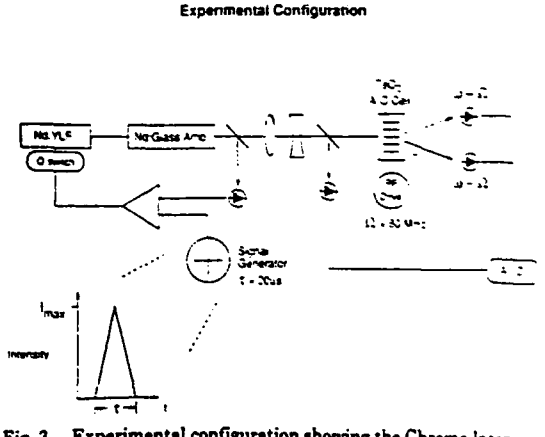

Fig. 3. Experimental configuration showing the Chroma laser system with closed loop control producing a triangular temporal pulse. The pulse is focused and collimated by the lenses shown and directed into the TeO_2 AO cell. Incident and diffracted intensities are monitored by photodiodes whose outputs are directed to an analog-to-digital (A/D) converter. Measurements are taken in this fashion in the two configurations yielding a frequency-upshifted and a frequency-downshifted diffracted beam (dotted and solid arrows, respectively).

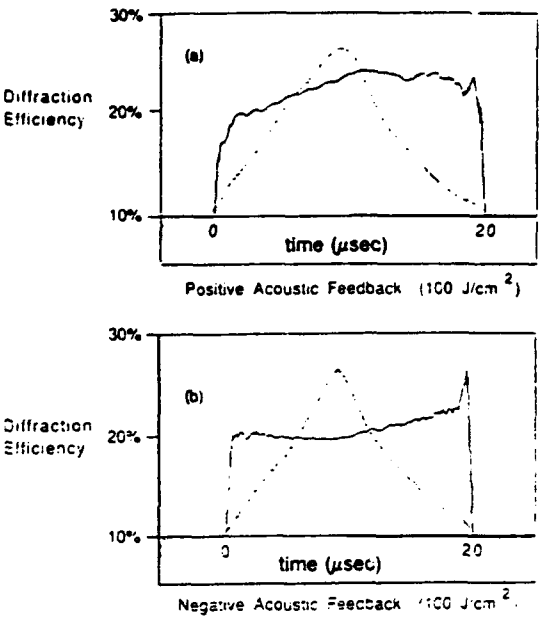

Fig. 4. (a) Time-resolved diffraction efficiency $\eta_{av}(t)$ (solid curve) and the incident intensity $I(t)$ (dotted curve) versus time for a peak intensity of 10 MW/cm^2 in the frequency-downshifted (i.e., positive-feedback) configuration. Note the roughly triangular response and the peak efficiency of 24%. (b) Time-resolved diffraction efficiency $\eta_{av}(t)$ (solid curve) and the incident intensity $I(t)$ (dotted curve) versus time for a peak intensity of 10 MW/cm^2 in the frequency-upshifted (negative-feedback) configuration. Note inverse triangular response.

The results of these measurements at the highest incident intensity before damage occurred are presented in Figs. 4(a) and 4(b) for the two diffraction configurations. In both of these figures the diffraction efficiency $\eta_{av}(t)$ (solid curves) and the incident intensity $I(t)$ (dotted curves) are plotted versus time during the optical pulse. Both figures were obtained by averaging the results of three pulses at a total pulse energy of 1 J corresponding to a peak incident intensity of roughly 10 MW/cm^2. The data presented in Fig. 4(a) were taken in the configuration in which the diffracted beam is frequency downshifted (adding energy to the acoustic wave) and those shown in Fig. 4(b) in the alternative frequency-upshifted configuration. Comparing these two plots, we see that in both cases the diffraction efficiency is 20% at the onset of the pulse. In the downshifted configuration shown in Fig. 4(a) the diffraction efficiency ramps up to a maximum of roughly 24% slightly past the midpoint of the pulse, followed by a noisier and slower decrease to approximately 22–23% by the end of the pulse. In comparison, the upshifted data in Fig. 4(b) show a slow downward ramp to ~19% near the pulse midpoint followed by a more rapid rise to ~23% by the end of the pulse.

Comparing these two results, we see that, indeed, there is some triangular waveform roughly proportional to the incident intensity pulse shape superimposed upon the diffraction efficiency, though with a slight delay between the peaks in $I(t)$ and $\eta_{av}(t)$ owing to the transit-time-time averaged nature of the response as described by expression (29). Additionally, the sign of this modification depends on the sign of the frequency shift, as predicted by our theoretical analy-

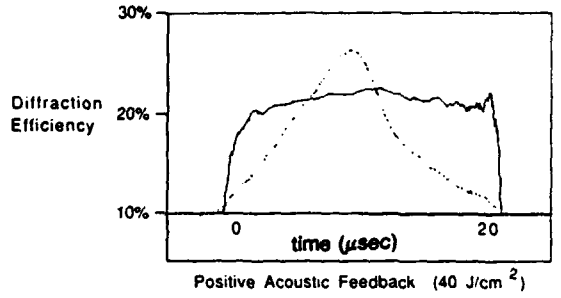

Fig. 5. Time-resolved diffraction efficiency $\eta_{av}(t)$ (solid curve) and the incident intensity $I(t)$ (dotted curve) versus time for a peak intensity of 4 MW/cm^2 in the frequency-downshifted (i.e., positive-feedback) configuration. Note the apparent absence of the monotonically increasing trend in $\eta_{av}(t)$ found in the higher-intensity results.

sis. Further, we note that the maximum increase in the diffraction efficiency is roughly 4% added to a background level of 20% and thus corresponds to a total enhancement of 20% at the maximum incident intensity of 10 MW/cm^2. Using Eq. (30) and assuming that the shape of the illuminated spot is roughly Gaussian, we see that we would expect a peak diffraction enhancement of $I_{max}/(2\sqrt{2}I_{threshold})$. As the calculated threshold for this process is $I_{threshold}$ = 19 MW/cm^2, our peak incident intensity of I_{max} = 10 MW/cm^2 implies a predicted enhancement level of 19%, which agrees quite well with the 20% degree of enhancement observed.

We note, however, that along with the directly intensity-dependent behavior that we predicted, both curves show an apparent asymmetry about the extremum in $\eta_{av}(t)$ corresponding to an additional monotonically increasing trend not accounted for in our analysis. We believe this to be a manifestation of thermally induced optical nonlinearities within the medium. Although our analysis ignoring such effects is reasonably accurate at lower intensities, as we approach the optical damage threshold these competing effects become significant. We justify this contention that such competing nonlinearities are relatively unimportant well below the damage threshold by presenting results analogous to those shown in Fig. 4(a) but at lower incident intensity. These results, presented in Fig. 5, correspond to measurements of $\eta_{av}(t)$ and $I(t)$ in the frequency-downshift configuration that was used in Fig. 4(a), again averaged over three data sets but now taken at an incident intensity of 4 MW/cm^2. Examining this figure, we see that there is again some evidence of the intensity-dependent triangular waveform superimposed upon the diffraction efficiency plot—but of approximately half the magnitude of that seen in Fig. 4(a), as we would expect from the reduced intensity. More importantly, there is only minimal evidence of monotonic ramping in this plot, indicating that indeed this effect becomes significant only as the damage threshold is neared.

4. DISCUSSION

As claimed, we have presented evidence of intensity-dependent enhanced diffraction in an AO device and have shown that the magnitude of the effect that we observed agrees well with that predicted in our earlier theoretical analysis. Clearly, though, as we were able to show only a 20% improvement in diffraction efficiency at incident intensities nearing the damage threshold of the device, the practical utility of this effect as demonstrated is limited. The large increases in diffraction efficiency predicted by our theory and the earlier analysis of Yeh and Khoshnevisan should, however, be achievable through more sophisticated control of the experimental conditions.

Specifically, we recall from Subsection 2.D that the threshold for nonlinear enhancement depends critically on the temporal and geometric properties of the pulse, with optimal thresholds achieved by increasing the transverse beam width D_x to approximately the acoustic attenuation length L_{ac}. As the attenuation length for TeO_2 operated in the slow-shear mode exceeds 1 cm,[10] we were thus quite far from this optimum in the initial experiments reported herein. If a transducer with a sufficiently large clear aperture is obtained and our spot size of 1 mm in these experiments is increased to this level, we may expect threshold reductions of greater than an order of magnitude. Since such reductions are associated with no concomitant alteration in the damage threshold of the medium, this modification should allow for high efficiency enhancement well above the threshold. Such modifications to our experiment are currently in progress, and the results will be reported in a subsequent publication.

APPENDIX A: SOLUTION FOR THE OPTICALLY DRIVEN DENSITY WAVE

In Section 2 we derived Eq. (8) describing the evolution of the optically induced acoustic field and then stated, without proof, its solution. In this appendix we derive the solution to this equation and, in so doing, elucidate the approximations made in obtaining our earlier result. We recall from Section 2 that Eq. (8) was a linear damped wave equation with an inhomogeneous forcing term, which could be expressed as

$$-d^2(\Delta\rho_{opt})/dt^2 + v^2\nabla^2(\Delta\rho_{opt}) + (2v^3/\Omega^2 L_{ac})\frac{d}{dt}\nabla^2(\Delta\rho_{opt}) \approx \frac{1}{4\pi}\gamma\nabla^2[f(\mathbf{r}, t)\exp[i\Omega(x/v - t)] + \text{c.c.}], \quad \text{(A1)}$$

where the driving term $f(\mathbf{r}, t)$ above is the interference term in the optical intensity and, for notational convenience, Ω may be positive or negative. Taking the Fourier transform of this equation with respect to position, we obtain the ordinary differential equation

$$P_{tt}(\mathbf{k}, t) + 2\Gamma(k)P_t(\mathbf{k}, t) + v^2k^2P(\mathbf{k}, t) = \frac{1}{4\pi}\gamma k^2 F\left(\mathbf{k} - \frac{\Omega}{v}\hat{x}, t\right)\exp(-i\Omega t), \quad \text{(A2a)}$$

where $\Gamma(k) \equiv v^3k^2/\Omega^2L_{ac}$ is the acoustic damping rate and, as before, $\hat{x}$ is a unit vector in the acoustic propagation direction. Here we have made the transform definitions

$$\Delta\rho_{opt}(\mathbf{r}, t) = 1/(2\pi)^3\left[\int P(\mathbf{k}, t)\exp(i\mathbf{k}\cdot\mathbf{r})d\mathbf{k} + \text{c.c}\right] \quad \text{(A2b)}$$

and

$$f(\mathbf{r}, t) = 1/(2\pi)^3\int F(\mathbf{k}, t)\exp(i\mathbf{k}\cdot\mathbf{r})d\mathbf{k}. \quad \text{(A2c)}$$

We now identify Eq. (A2a) as a simple driven oscillator equation with the solution

$$P(\mathbf{k}, t) = (\gamma k^2/4\pi\Omega_1)\exp(-i\Omega t)\int_0^\infty F[\mathbf{k} - (\Omega/v)\hat{x}, t - s] \times \exp([i\Omega - \Gamma(k)]s)\sin(\Omega_1 s)ds, \quad \text{(A3)}$$

where $\Omega_1(k) \equiv vk[1 - [\Gamma(k)/vk]^2]^{1/2}$ is the natural frequency of the damped oscillator. We now take the inverse transform by substituting Eq. (A3) into Eq. (A2b) and exchanging the orders of integration to obtain

$$\Delta\rho_{opt}(\mathbf{r}, t) = (\gamma/32\pi^4)\left\{\exp[i\Omega(x/v - t)]\int_0^\infty ds\,\exp(i\Omega s) \times \int d\mathbf{k}_1(k^2/\Omega_1)F(\mathbf{k}_1, t - s)\exp[i\mathbf{k}_1\cdot\mathbf{r} - \Gamma(k)s]\sin(\Omega_1 s) + \text{c.c.}\right\}, \quad \text{(A4)}$$

where $\mathbf{k}_1 \equiv \mathbf{k} - (\Omega/v)\hat{x}$ and hence $k = (\Omega/v)[1 + 2(v/\Omega)\mathbf{k}_1\cdot\hat{x} + (vk_1/\Omega)^2]^{1/2}$. We shall now assume that the driving function $f(\mathbf{r}, t)$ varies slowly on the scale of the acoustic wavelength, i.e., that the characteristic length scale $D \sim \max(D_x, D_y) \gg v/\Omega$, and note that, since $v/\Omega \approx 1\ \mu$m for TeO_2 in the slow-shear mode at our drive frequency of 80 MHz, this condition is easily satisfied. Making this assumption implies that $k_1 \sim O(2\pi/D)$ is small compared with k within the bandwidth of $F(\mathbf{k}, t)$ and allows us to write $k \approx \Omega/v$ outside the exponentials in Eq. (A4). In the exponential terms, however, in which functions of k may be multiplied by large factors, we must be somewhat more careful. Specifically, we note that to first order in k_1 we have

$$\Gamma(k) \approx (v/L_{ac})[1 + (2v/\Omega)\mathbf{k}_1\cdot\hat{x} \approx (v/L_{ac})(1 + 4\pi v/\Omega D_x). \quad \text{(A5)}$$

Hence, to replace $[\Gamma(k)s]$ by (vs/L_{ac}) in the exponential in Eq. (A4), the error term

$$\exp(-vs/L_{ac})4\pi v^2 s/\Omega D_x L_{ac} \quad \text{(A6)}$$

must be small compared to unity. Since this expression is maximized for $s = L_{ac}/v$, we see that assuming that $D_x \gg v/\Omega$ automatically satisfies this condition as well. Using this result, we see that we may write $\Omega_1(k) \approx vk$ in Eq. (A4). The argument of the sin term in this equation may thus be written as

$$\Omega_1 s = \Omega s + vs\mathbf{k}_1\cdot\hat{x} + O[s(vk_1)^2/\Omega]. \quad \text{(A7)}$$

We again use $k_1 \sim O(2\pi/D)$ and $s \sim L_{ac}/v$ (since the integrand falls off exponentially for larger s values) to evaluate the magnitudes of these terms. Making these substitutions, we see that the third term is small whenever the spot size D is large compared with $(vL_{ac}/\Omega)^{1/2} \approx 10^{-2}$ cm for TeO_2 under the conditions that we have examined. Thus, while this condition is considerably more restrictive than the earlier requirement of $D \gg v/\Omega$, it is still easily satisfied. The second term in Eq. (A7), however, is of the order of $2\pi L_{ac}/D$, which is much larger than unity under the experimental conditions that we have considered. Both of the first two terms in Eqs. (A7) are thus required for our evaluation of Eq. (A4) to remain accurate.

Making the series of approximations described above, we may rewrite Eq. (A4) as

$$\Delta\rho_{opt}(\mathbf{r}, t) = (\gamma\Omega/8\pi iv^2)\Big(\exp[i\Omega(x/v - t)] \times \int_0^\infty ds\,\exp(i\Omega s)\exp(-vs/L_{ac}) \times 1/(2\pi)^3\Big\{\int d\mathbf{k}_1 F(\mathbf{k}_1, t - s)\exp[i\mathbf{k}_1\cdot(\mathbf{r} + vs\hat{x}) + i\Omega s] - \int d\mathbf{k}_1 F(\mathbf{k}_1, t - s)\exp[i\mathbf{k}_1\cdot(\mathbf{r} - vs\hat{x}) - i\Omega s]\Big\} + \text{c.c.}\Big). \quad \text{(A8)}$$

The latter two integrals in this expression are now recognized as Fourier transforms with traveling-wave kernels and may be evaluated by using Eq. (A2c). Performing these integrations yields the result of Eq. (9) in Section 2, as claimed.

ACKNOWLEDGMENTS

The authors thank the staff of KMS Fusion in Ann Arbor, Michigan, and in particular N. K. Moncur, R. Maynard, and R. P. Johnson, whose assistance was instrumental in our conducting the experiments described herein. We also gratefully acknowledge the support of the U.S. Office of Naval Research under contract N00014-88-C-0231.

REFERENCES

1. A. Yariv and P. Yeh, *Optical Waves in Crystals* (Wiley, New York, 1984).
2. W. Kaiser and M. Maier, in *Laser Handbook*, F. T. Arecchi and E. O. Schulz-Dubois, eds. (North-Holland, Amsterdam, 1972), pp. 1077–1150.
3. A. Korpel, R. Adler, and B. Alpiner, "Direct observation of optically induced generation and amplification of sound," Appl. Phys. Lett. 5, 86–88 (1964).
4. D. E. Caddes, "Parametric interaction of light with acoustic waves," Ph.D. dissertation (Stanford University, Stanford, Calif., 1966).
5. P. Yeh and M. Khoshnevisan, "Nonlinear optical Bragg scattering in Kerr media," J. Opt. Soc. Am. B 4, 1954–1957 (1987).
6. H. Kogelnik, "Coupled wave theory for thick hologram gratings," Bell Sys. Tech. J. 48, 2909–2947 (1969).
7. N. M. Kroll, "Excitation of hypersonic vibrations by means of photoelastic coupling of high intensity light waves to elastic waves," J. Appl. Phys. 36, 34–43 (1965).
8. G. N. Watson, *A Treatise on the Theory of Bessel Functions*, 2nd ed. (Cambridge U. Press, Cambridge, 1944).
9. R. P. Johnson, N. K. Moncur, and L. D. Siebert, "Output pulse shape control on a high power solid-state laser using electronic feedback," in *Proceedings of the International Conference on Lasers* (American Chemical Society, Washington, D.C., 1988), pp. 432–436.
10. N. Uchida and Y. Ohmachi, "Elastic and photoelastic properties of TeO_2 single crystal," J. Appl. Phys. 40, 4962–4965 (1969).

Efficient optical enhancement of acousto-optic diffraction using optimized overlap of coupled waves

Frederick Vachss and Ian McMichael

Applied Optics Department, Rockwell International Science Center, 1049 Camino Dos Rios, Thousand Oaks, California 91360

Received February 5, 1990; accepted May 10, 1990

We describe a technique by which the diffraction efficiency of an acousto-optic beam deflector may be substantially increased under high-power laser illumination. In earlier research we showed that the diffraction process is intrinsically associated with an intensity-dependent modification of the diffraction efficiency of an acousto-optic device. Here we show that this diffraction efficiency may be enhanced most effectively by distributing the optical intensity over the acousto-optic device in a manner that maximizes the overlap with the acoustic wave in the medium. In particular, we demonstrate increases in diffraction efficiency of greater than 80% in a TeO_2 device—an improvement of roughly an order of magnitude over earlier results in which this overlap technique was not used.

The deflection of a laser beam using acousto-optic (AO) diffraction was first achieved over two decades ago and has since evolved into a commonly used beam-steering technology. While AO deflection is effective in many situations, in certain applications the limitations of this technique become objectionable. In particular, in high optical power and high pointing accuracy applications the device aperture must be made large. This results in increasingly high acoustic power requirements, adding significantly to the size and weight of the device. We thus desire a means to reduce the acoustic power required to yield a given diffraction efficiency over a given aperture, or, equivalently, a means by which the effective value of M_2, the standard figure of merit characterizing the AO properties of a material, may be increased.

While the most direct approach to this problem is to search for or tailor a new material with more desirable AO properties (and indeed this is an ongoing area of research), we pursue an alternative mode of attack and amplify the acoustic wave within an existing device. This acoustic amplification occurs through the electrostrictive effect present in an AO medium and transfers power from the optical field incident upon the device to the acoustic wave within during the diffraction process as diagrammed in Fig. 1. Specifically, as was shown by Yeh and Khoshnevisan,[1] the intensity pattern generated by the interference of the incident and diffracted optical beams in an AO deflector travels along with the acoustic wave in the device, and hence the electrostrictively induced acoustic response of the medium to this intensity pattern adds coherently to the acoustic wave present and either amplifies or diminishes it. This acoustic amplification is a simple consequence of energy conservation, since the frequency shift between the incident and diffracted optical beams implies that for every photon diffracted from the acoustic grating an acoustic phonon must be added to (or removed from) the acoustic wave.

Since the electrostrictive response of any medium is intrinsically related to its photoelastic coefficients[2] (and hence to its AO properties), this amplification process occurs to some degree in all AO beam deflectors. The fact that this effect is not apparent in most situations implies that certain conditions must be met for appreciable acoustic amplification to be achieved. These conditions, along with a detailed theoretical explanation and a preliminary experimental demonstration of this effect, were described recently.[3]

In Ref. 3 we showed that by focusing a long-duration (20-μsec) laser pulse onto a TeO_2 AO beam deflector, a 20% peak improvement in the device diffraction efficiency could be achieved at a peak incident intensity of 10 MW/cm^2. This result was of limited practical use, however, since optical damage to the deflector occurred at similar intensity levels. In the theoretical analysis accompanying this result, however, we showed that the intensity required to achieve this optical enhancement depends strongly on the spatial distribution of this intensity on the device. Specifically, the optical intensity required for a given level of diffractive enhancement was shown to decrease with increasing transverse width of the laser spot in the direction of acoustic propagation shown in Fig. 1. This is a result of the traveling-wave nature of the acoustic wave within the device. When energy is added to the acoustic wave by the diffraction process, this energy then propagates along with the acoustic wave. Once

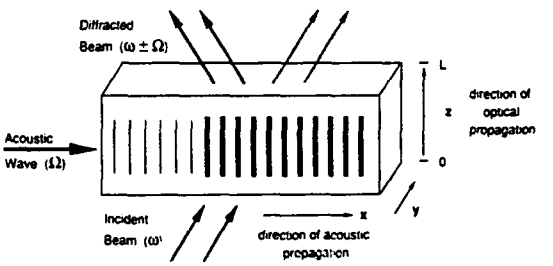

Fig. 1. Basic AO configuration showing the operating coordinate system, the directions of acoustic and optical propagation, and the modification of the acoustic intensity owing to optical diffraction. Note that the optically modified acoustic wave propagates out of the illuminated region.

0146-9592/90/160921-03$02.00/0

this energy propagates outside of the region of illumination, however, it no longer has any impact on the diffraction efficiency of the device and is wasted as far as the present application is concerned. By extending the incident optical beam in the direction of acoustic propagation we thus increase the degree of overlap between the amplified acoustic wave and the beam it must diffract. In this Letter we describe experiments conducted with such transversely extended optical beams and compare the results with those of the earlier focused-spot experiments. We show that not only are large improvements in the degree of enhancement achieved but that the gain in efficiency is large enough so that an increasingly nonlinear dependence of diffraction efficiency on incident intensity is observed.

In our earlier analysis of the enhancement process,[3] coupled equations were derived describing the interaction of the acoustic and optical waves within the medium. These equations were then solved in the regime of weak depletion of the incident optical beam (i.e., low diffraction efficiency) to obtain the following expression for the spatially averaged intensity-dependent diffraction efficiency of the AO device:

$$\eta_{av}(t) \equiv I_{\text{diffracted}}/I_0 \approx \eta_0 H^2[\pm I_0(t)/I_{\text{threshold}}], \qquad (1)$$

where $I_0(t)$ is the intensity of the optical beam incident upon the device, η_0 is the unamplified diffraction efficiency obtained from the device at low intensities, and $H^2(u)$ is a nonlinear gain function that grows linearly with unit slope for small arguments but grows exponentially for $u \gg 1$. The sign of the argument is determined by the sign of the frequency shift accompanying the diffraction process. For the case of acoustic amplification, in which the frequency of the diffracted optical beam is reduced from that of the incident beam, the positive sign is used. The negative sign is thus reserved for the corresponding deamplification process.

The threshold optical intensity characterizing this nonlinear response is expressed as

$$I_{\text{threshold}} \equiv \frac{1}{M_2}\frac{16\lambda c}{\pi n L \Omega D_x^2}, \qquad (2)$$

where M_2 is the AO figure of merit mentioned above, n and L are the refractive index and thickness of the medium, respectively, Ω is the acoustic driving frequency, λ and D_x are the wavelength and transverse spot size, respectively, of the incident optical beam, and c is the speed of light.

While Eq. (2) contains a variety of physical parameters that may be varied to minimize $I_{\text{threshold}}$, for a given AO material the factors M_2 and n are fixed and Ω and L are not easily varied once the device has been produced. Thus the threshold is modified most easily through control of the incident wavelength and spot size. Since second-harmonic generation was not easily achievable with the laser systems that were available, we elected to modify the transverse spot size D_x to attempt to lower the threshold for diffractive enhancement. In examining Eq. (2), it appears that the threshold can be driven arbitrarily low by increasing D_x without bound. Clearly, this is incorrect and is in fact a manifestation of the approximations used in obtaining this expression. Specifically, our threshold expression is only strictly valid when D_x is much less than L_{ac}, the acoustic attenuation length in the medium. When the spot size approaches or exceeds the attenuation length, the threshold approaches a limiting value obtained by replacing D_x by L_{ac} in Eq. (2) above. Thus by increasing the transverse spot size from an initial value of $D_x = D_{x0}$ to $D_x = L_{ac}$ we may achieve a reduction in our intensity threshold of the order of D_{x0}/L_{ac}. Applying this result to the experimental system considered in our earlier research,[3] in which a 1-mm^2 focused spot was used to illuminate a TeO_2 deflector with an attenuation length of roughly 1 cm, we see that a reduction in $I_{\text{threshold}}$ approaching an order of magnitude should be possible simply by increasing the spot size.

To test this hypothesis, we used an experimental setup similar to that employed in the earlier focused-spot research (Fig. 2). Here a high-power Nd:YLF oscillator/Nd:glass amplifier system developed at KMS Fusion was used to generate a 1.05-μm pulse 20 μsec in duration, with such long pulses being necessary to achieve significant nonlinear gain. By using an electronic feedback system developed at KMS, the temporal profile of this pulse was forced to follow a triangular wave form as shown. This pulse was then sent through anamorphic optics to result in a collimated beam 1 mm in height and 1 cm in width with a nearly uniform transverse profile incident upon a TeO_2 AO deflector. The deflector was oriented at the Bragg angle to maximize AO diffraction of the incident pulse. The total incident and diffracted powers were then monitored in real time to give a measurement of the spatially averaged diffraction efficiency, $\eta_{av}(t)$, during the pulse. These measurements were carried out in both deflector orientations, yielding an upshift and a downshift of the frequency of the diffracted light with respect to that of the incident pulse. From relation (1) above we see that these two diffractive configurations should yield nonlinear-optical responses of opposite sign, with the frequency-upshifted case, in which energy is carried away from the acoustic wave, yielding a reduction in diffraction efficiency and the frequency-downshift case conversely resulting in acoustic amplification.

Measurements of $\eta_{av}(t)$ in both these configurations were carried out at increasing pulse intensities until optical damage to the deflector resulted. The maximum incident intensity achieved before damage resulted was 5.7 MW/cm^2. The data taken at this intensity level in both diffractive orientations are plotted in

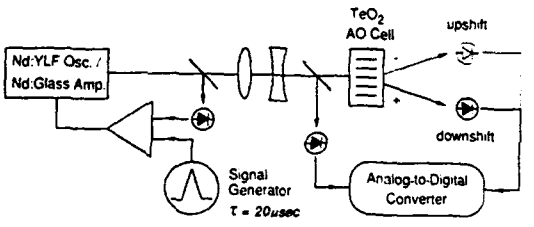

Fig. 2. Experimental setup showing the YLF laser source, the pulse-shaping system, and the TeO_2 AO cell. Real-time intensities are monitored with photodiodes, whose outputs are digitized and stored.

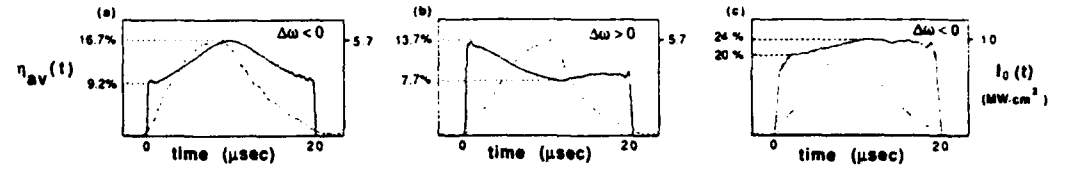

Fig. 3. Plots of $\eta_{av}(t)$ (solid curves, scales on left) and $I_0(t)$ (dotted curves, scales on right) versus time during the optical pulse. (a), (b) Reponse using a 1-cm transverse spot width with a 5.7-MW/cm^2 peak intensity in the frequency-downshift (amplifying) configuration and the converse frequency-upshift (deamplifying) configuration, respectively. (c) Response in the amplifying configuration using a 1-mm^2 focused spot and a peak intensity of 10 MW/cm^2. Note the reduction in enhancement of (c) compared with (a).

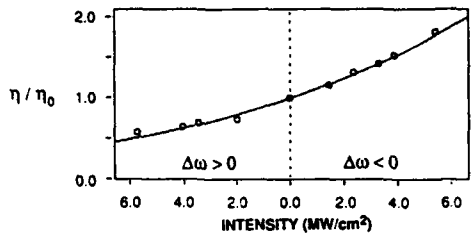

Fig. 4. Extremum values of $\eta_{av}(t)/\eta_0$ versus peak incident intensity (open circles) along with a least-squares fit of the theoretical gain function $H^2(I_0/I_{threshold})$ using $I_{threshold}$ as a curve-fitting parameter. Intensity values in the deamplifying configuration are plotted as negative quantities following the convention of Eq. (1).

Figs. 3(a) and 3(b). Here $\eta_{av}(t)$ (solid curves) and the incident intensity pulse $I_0(t)$ (dotted curves) are plotted versus time during the 20-μsec pulse. We see in the frequency-downshift case shown in Fig. 3(a) that a substantial positive triangular wave form is superimposed onto $\eta_{av}(t)$ with the initial diffraction efficiency of roughly 9% almost doubling to a peak value of 17% at mid-pulse. Conversely, in the alternative case of frequency upshift shown in Fig. 3(b), an inverted triangular wave form is present in the efficiency data with the initial value of nearly 14% reduced to less than 8% at mid-pulse. Since the incident intensity $I_0(t)$ is a triangular pulse, we see from relation (1) that this similar triangular behavior in $\eta_{av}(t)$ is evidence of the intensity-dependent diffraction effect that we wish to demonstrate. The fact that the sign of this triangular behavior exhibits the predicted dependence on the sign of the diffractive frequency shift is particularly convincing evidence of this effect.

To evaluate the impact of our transverse extended beam technique, for comparison Fig. 3(c) shows a similar data set of $\eta_{av}(t)$ and $I_0(t)$ taken from our earlier research[3] using a 1-mm^2 focused spot at a peak intensity of 10 MW/cm^2. We see here that although the increasing triangular behavior is indeed still present, it is substantially weaker, with a growth only to 24% from an initial value of 20% shown. This 20% gain in the diffraction efficiency is less than one fourth of the 80–85% gain demonstrated in the extended beam result of Fig. 3(a). This is all the more striking given that the results in Fig. 3(a) were obtained at slightly more than half the intensity used in the focused-spot results. Thus in terms of fractional improvement in diffraction efficiency per unit of incident intensity, we do indeed improve on our earlier results by a factor of 7 to 8—nearly the order of magnitude predicted earlier.

We note in examining the data presented above that while the peak efficiency is increased by roughly 83% in the acoustic amplification configuration shown in Fig. 3(a), the efficiency is only reduced by a factor of 45% in the corresponding deamplification case in Fig. 3(b). This asymmetry is a manifestation of the nonlinear nature of the gain function $H^2(u)$ in relation (1). To demonstrate this we measured $\eta_{av}(t)$ over a range of intensities in both diffractive orientations, and from these data we computed the ratio between the extremum in efficiency and its initial value η_0. These ratios are plotted versus the peak incident intensity I_0 in Fig. 4. Along with these data points is a plot of $H^2(I_0/I_{threshold})$ using $I_{threshold}$ as a free parameter and the exact form of H^2 developed in our earlier paper. Following the convention of relation (1), the intensity data in the configuration yielding acoustic deamplification are plotted as negative numbers. Examining this plot, we see that the agreement between the predicted and observed intensity dependence is quite good and that the result of our least-squares fit to the data is an effective intensity threshold of $I_{threshold} \approx 9.3 \pm 0.6$ MW/cm^2. Thus while the nonlinear nature of the gain function is apparent in this plot, we see that all our data were taken with peak intensities below the measured threshold. Since $H^2(u)$ increases exponentially for $u > 1$, however, this implies that even small further reductions in $I_{threshold}$ could permit this threshold to be exceeded and result in substantial improvements in the degree of enhancement observed at the incident intensity levels that we have used. In particular, from Eq. (2) we see that by using a thicker AO device and perhaps by increasing the frequencies of the acoustic and optical waves, such further reductions in the threshold should be achievable, permitting the regime of exponentially increasing intensity-dependent efficiency to be reached. Attempts to further reduce the threshold in this manner are currently in progress and will be reported in a future publication.

The authors acknowledge the support of the U.S. Office of Naval Research under contract N00014-88-C-0231.

References

1. P. Yeh and M. Khoshnevisan, J. Opt. Soc. Am. B 4, 1954 (1987).
2. W. Kaiser and M. Maier, in *Laser Handbook*, F. T. Arecchi and E. O. Schulz-Dubois, eds. (North-Holland, Amsterdam, 1972), pp. 1077–1150.
3. F. Vachss, I. McMichael, M. Khoshnevisan, and P. Yeh, J. Opt. Soc. Am. B 7, 859 (1990).

Observation of high-gain nonlinear acousto-optic amplification

Frederick Vachss and Ian McMichael

Applied Optics Department, Rockwell International Science Center, Thousand Oaks, California 91360

Received October 28, 1991

We describe a procedure by which the optical and acoustic waves present in an acousto-optic beam deflector are strongly amplified through nonlinear optical pumping. This amplification is manifested as an increase in the diffraction efficiency of an acousto-optic beam deflector. In particular, we describe the design and experimental test of a prototype TeO_2 device in which this diffraction efficiency was increased by more than 2 orders of magnitude under pulsed laser illumination. This high degree of amplification results from an acoustic gain mechanism that counteracts the usual attenuation of sound waves propagating in an acousto-optic medium. We discuss possible applications of this gain mechanism in a new class of nonlinear acousto-optic device.

Acousto-optic (AO) devices provide a convenient means by which optical beams may be modulated or steered and thus have found use in a wide variety of applications ranging from signal processing to image reproduction. The same phenomenon that allows for the diffraction of light by sound in these applications, however, also provides a mechanism for nonlinear optical response in AO devices. Specifically, the photoelastic effect in a medium, which causes a variation in the medium's refractive index in proportion to an acoustic perturbation, implies the existence[1] of a corresponding electrostrictive effect, causing an acoustic response in the medium proportional to the square of the local electric field. In particular, this correspondence implies that materials with a high AO figure of merit, M_2 (i.e., a large variation in refractive index for a given acoustic intensity), will possess a strong nonlinear-optical response through which acoustic waves may be excited by mixing optical beams within the material.

Previously we have shown[2] that this nonlinear response may be used to enhance the diffraction efficiency of an AO beam deflector. In such a device, as depicted in Fig. 1, an incident optical beam diffracts from the refractive-index field generated by an acoustic wave in a photoelastic medium and gives rise to a second optical beam. Through the corresponding nonlinear electrostrictive response, the two optical beams then mix in the medium and produce an acoustic wave driven by the product of these two optical fields. Because the optical interference pattern travels along with the acoustic wave in the material, this optically generated acoustic wave propagates along with the acoustic wave already present in the material, and the two add coherently. This nonlinear process thus amplifies the acoustic wave in the material and increases the diffraction efficiency of the device.

In the first demonstrations of this effect, we found that whereas diffraction efficiencies could be improved by using focused illumination from a high-powered pulsed laser, measurable effects only occurred at optical intensities near the damage threshold of the AO material. Analysis of these results, however, led to improved experimental techniques by which such enhancements in efficiency could be obtained with substantially reduced intensities.[3] Specifically, it was found that such nonlinear effects would become large whenever the optical intensity exceeded a threshold value given by

$$I_t \equiv \frac{1}{M_2}\frac{16\lambda c}{\pi n \Omega L D_x}, \tag{1}$$

where M_2 is the AO figure of merit mentioned above, n and L are the refractive index and thickness of the medium, respectively, Ω is the acoustic driving frequency, λ is the optical wavelength, and D_x is the width of the optical beam in the direction of acoustic propagation. This last factor implies that increasing the optical beam width results in a proportional decrease in the threshold intensity. Indeed, improvements in diffraction efficiency roughly an order of magnitude greater than those seen in the initial demonstrations with focused spot illumination were obtained by using optical beams covering the full width of an AO deflector.[3] Even in this latter study, however, nonlinear gain in diffraction efficiency of less than a factor of 2 was achieved before the optical damage level was reached. Furthermore this damage threshold occurred at an intensity slightly lower

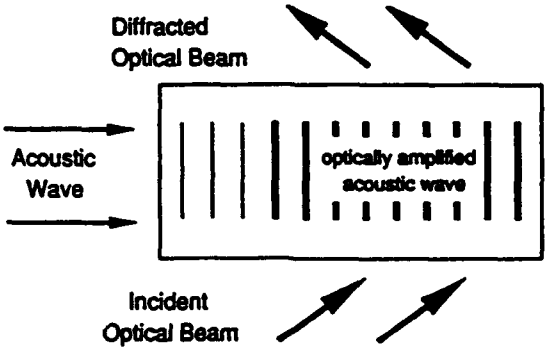

Fig. 1. Diagram of AO beam deflector showing the interacting acoustic and optical waves and the amplification of the acoustic intensity that is due to optical diffraction.

0146-9592/92/060453-03$5.00/0

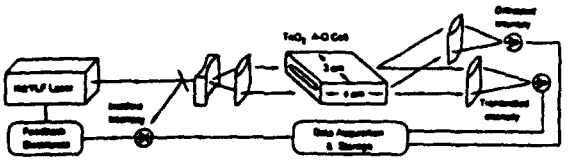

Fig. 2. Experimental setup showing the laser source, the feedback pulse-shaping system, and the 1 cm × 3 cm × 4 cm TeO_2 AO cell. Real-time intensities of the incident, transmitted, and diffracted optical beams are monitored by using photodiodes, whose outputs are digitized and stored.

than I_t, clearly limiting any potential application of this effect. In this Letter we demonstrate techniques to reduce I_t sufficiently so that substantial nonlinear response is seen at intensities well below the damage level. We then describe several applications of this AO nonlinearity.

From Eq. (1) we see that I_t is proportional to the factor $(LD_z)^{-1}$ and thus varies inversely with the total area over which the crossed acoustic and optical beams interact. We may thus reduce the nonlinear threshold simply by using a larger AO device. As the large interaction areas at which nonlinear AO effects become significant are not needed in standard commercial AO devices, however, we designed and commissioned the fabrication of a prototype AO beam deflector, using TeO_2 as the medium for its high value of M_2 as in previous research. The dimensions of this device, however, are 3 cm × 4 cm in the acoustic and optical propagation directions, respectively, compared with the 1 cm × 0.6 cm interaction region of the off-the-shelf device used in our earlier demonstrations. The device thickness was determined by both the availability of sufficiently large starting crystals and the need to maintain a uniform acoustic wave front. Given a device of these dimensions, to take full advantage of the overlapping acoustic and optical beams, we must illuminate the device with an optical pulse of duration equal to the transit time for the acoustic wave across the device aperture. For our 3-cm aperture and the 6×10^4 cm/s acoustic velocity of TeO_2, this implies a pulse duration of 50 μs. Additionally Eq. (1) implies that the acoustic driving frequency Ω should be as high as possible to minimize I_t. Because the attenuation length for acoustic waves in TeO_2 varies as the inverse square[4] of Ω, however, the effective aperture is limited if Ω is too large. In practice, choosing Ω so that the device aperture is roughly equal to the attenuation length yields the optimal response, in our device obtained at a driving frequency of 70 MHz.

Applying these criteria, we tested the nonlinear response of this device by using the apparatus depicted in Fig. 2. Here a Nd:YLF laser system capable of producing 1.05-μm pulses up to 20 J in energy with durations up to 200 μs illuminates the device. The temporal profile of the pulse is constrained to follow a square waveform through an electronic feedback system[5] connected to a Q switch in the laser cavity. The laser output is anamorphically expanded to produce a collimated beam with a Gaussian profile 1 mm in height but several centimeters in width at the surface of the device and oriented so that the long axis of the beam is parallel to the direction of acoustic propagation. This beam is then truncated in width to provide a uniform intensity profile over the device aperture. The device is aligned so that the optical beam is incident at the Bragg angle for maximum diffraction, and the light experiences a frequency downshift equal to the acoustic frequency during the diffraction process. This ensures that the diffraction process transfers energy from the incident optical beam to the acoustic wave in the medium, allowing for nonlinear amplification. After passage through the AO device, the optical beams propagate undisturbed for roughly 1 m to allow for spatial separation between the diffracted and undiffracted components. Both of these output components (as well as a small fraction of the light incident on the device) are then attenuated and focused onto calibrated photodiodes. The photodiode signals are monitored during each optical pulse, digitized, and stored, which yields time-resolved measurements of the intensities of the various beams. In particular, the time-resolved (but spatially averaged) diffraction efficiency of the device, $\eta_{av}(t)$, is determined from the point-by-point ratio of the diffracted and incident intensities.

Because the acoustic wave in the material interacts with an increasing fraction of the incident optical beams as it propagates across the device, the diffraction efficiency should increase during the period of illumination if nonlinear amplification is occurring. In particular, $\eta_{av}(t)$ should grow until the pulse duration exceeds the transit time of the acoustic wave across the illuminated aperture and remain constant thereafter. Because such growth may be limited if significant depletion of this incident optical beam occurs, the acoustic drive power was set sufficiently low so that η_0, the diffraction efficiency

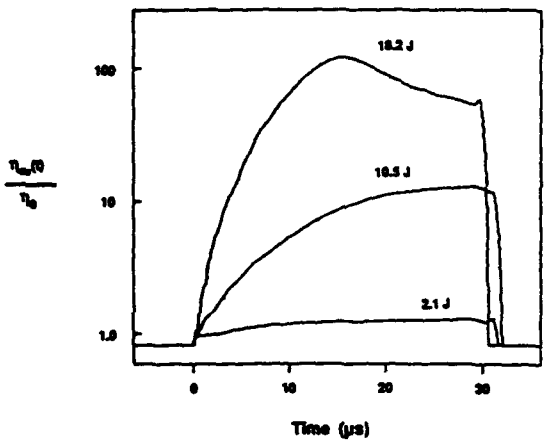

Fig. 3. Plots of spatially averaged diffraction efficiency $\eta_{av}(t)$ versus time during the optical pulse at incident energies of 2.1, 10.5, and 18.2 J. Note that the vertical axis is scaled logarithmically so that the maximum gain varies roughly exponentially with energy. Also note the nonmonotonic behavior of the highest energy curve, which indicates the presence of competing nonlinear phenomena.

of the device when probed with low-energy pulses from the laser source, was 0.11%.

Our experiment consisted of measuring the time-resolved diffraction efficiency for various incident-pulse energies. In all cases the qualitative behavior described in the preceding paragraph was observed, with growth of $\eta_{ac}(t)$ from an initial value of η_0. While a pulse duration equal to the aperture transit time of 50 μs was used in our initial measurements, we found that efficiencies near steady state were reached within 30 μs in all cases, and subsequent data were taken by using this reduced duration. Plots of $\eta_{ac}(t)$ for three values of incident-pulse energy are shown in Fig. 3. Whereas at the lowest incident energy of 2.1 J we see that $\eta_{ac}(t)$ is nearly constant during the pulse, growing to a maximum value only 1.3 times η_0, the higher energies give rise to much larger increases in diffraction efficiency. In particular, the maximum value of $\eta_{ac}(t)$ achieved during the pulse grows almost exponentially with incident energy, reaching a value of 12.4 times η_0 for a 10.5-J input pulse and 110 times η_0 for our maximum energy of 18.2 J.

This nearly exponential growth is typical of operation above the nonlinear threshold intensity given in Eq. (1). The exact expression for the gain in diffraction efficiency is given as[3]

$$G = I_1^2[2(I_{inc}/I_t)^{1/2}]/(I_{inc}/I_t), \qquad (2)$$

where G is the ratio between the maximum value of $\eta_{ac}(t)$ and η_0, I_{inc} is the incident intensity (assuming a constant temporal profile as has been used here), and I_1 is the first-order modified Bessel function, which indeed behaves exponentially for large values of the argument.[6] To determine the value of I_t achieved in our device, Eq. (2) was fitted to experimental values of G for several values of incident intensity by using I_t as a free parameter. This comparison yielded a value of $I_t = 0.33 \pm 0.04$ MW/cm^2, almost 30 times smaller than the threshold value of 9.3 MW/cm^2 obtained in our previous experiments. Because our maximum input energy of 18.2 J corresponds to an intensity of 2.0 MW/cm^2, the value of I_t obtained here implies that we have exceeded our nonlinear threshold by a factor of 6. Furthermore, because the threshold for optical damage in TeO_2 has been determined to be 5–10 MW/cm^2, we have achieved this high-gain operation without risk of damage. The maximum pulse energy used in our experiments was thus determined by available laser power rather than by damage limits as in previous research.

Operation at intensities well in excess of I_t, however, does cause other phenomena that may limit the achievable nonlinear response even if optical damage does not do so. In particular, at incident intensities above 3 to 4 times I_t, we observed depletion of the incident optical beam exceeding any rise in the diffracted output intensity. This depletion of the undiffracted beam reduces the amount of light available for diffraction via the acoustic grating and is responsible for the falloff in diffractive enhancement seen in the latter portion of the 18.2-J data shown in Fig. 3. Whereas the cause of this depletion remains uncertain, the fact that this process occurs on the same time scale as the diffractive enhancement that we observe suggests a similar mechanism. Specifically, because the diffraction process presents such a strong gain mechanism for the acoustic wave already present in the medium, gain may be provided for other acoustic waves in the plane of illumination as well. In a process analogous to photorefractive beam fanning,[7] scattered light thus may mix with the undiffracted beam, generate additional acoustic waves in the material, and undergo amplification through the very nonlinear mechanism that we have optimized in our device.

Whereas such competing processes may provide an ultimate limit on the amount of nonlinear AO gain that we may achieve, a variety of interesting applications are still possible within the limitations thus imposed. The combination of high diffraction efficiency and reduced acoustic power requirements that we have demonstrated with large acoustic apertures makes this effect uniquely suitable for the remote steering of high-power laser beams with high diffraction-limited pointing accuracy. Moreover the gain process provided by this effect compensates somewhat for the attenuation experienced by acoustic waves in a medium. Indeed, for incident intensities well above threshold, the acoustic amplitudes grow quasi-exponentially[2] rather than decay during propagation. Thus by using this optical pumping technique it should be possible to create AO devices with acoustic apertures significantly larger than the usual acoustic attenuation length in a given medium and thus realize higher time–bandwidth products than have heretofore been obtained. Indeed, if the gain region is enclosed in an acoustic resonator, optically pumped acoustic oscillation should be achievable. Finally, our results indicate that AO materials may be used in a wide variety of nonlinear-optical applications such as beam coupling and phase conjugation if the long-pulse-duration, extended-spot-size techniques that we have developed are used. Demonstrations of such applications in these materials are the subject of our current research.

The authors acknowledge the support of the U.S. Office of Naval Research under contract N00014-88-C-0231.

References

1. M. Khoshnevisan and P. Yeh, Proc. Soc. Photo-Opt. Instrum. Eng. **739**, 82 (1987).
2. F. Vachss, I. McMichael, M. Khoshnevisan, and P. Yeh, J. Opt. Soc. Am. B **7**, 859 (1990).
3. F. Vachss and I. McMichael, Opt. Lett. **15**, 921 (1990).
4. N. Uchida, J. Appl. Phys. **43**, 2915 (1972).
5. R. P. Johnson, N. K. Moncur, and L. D. Siebert, in *Proceedings of International Conference on Lasers* (American Chemical Society, Washington, D.C., 1988), pp. 432–436.
6. F. W. J. Olver, in *Handbook of Mathematical Functions*, M. Abramowitz and I. A. Stegun, eds. (Dover, New York, 1965), pp. 358–433.
7. R. Vazquez, F. Vachss, R. Neurgaonkar, and M. Ewbank, J. Opt. Soc. Am. B **8**, 1932 (1991).

System Applications of Nonlinear Acousto-Optics (Kerr-Bragg) for Rapid Optical Beam Steering (ROBS)

In this section, the technical background of beam steering techniques and how Rockwell's studies will address the problem of using nonlinear optical phenomena for agile beam steering of high-energy laser beams will be described. Some of the studies were in collaboration with our Rocketdyne division, the details of which will not be discussed here, since they were supported outside of this program. What is described below is for the purpose of illustrating the relevance of this program's accomplishments for future system applications.

Background

This Rockwell study for Rapid Optical Beam Steering (ROBS) is based upon a nonlinear optical two-wave mixing process that will substantially alleviate many prior difficulties in the application of acousto-optical Bragg scattering to beam deflection of large, high-power lasers. It also offers a natural complement to other beam steering techniques that may be best suited to low-power applications (e.g., liquid crystal light valves and waveguides).

The use of acousto-optic (AO) beam steering devices for BMDO (SDI) applications is very desirable in terms of the generic device capabilities. In AO beam steering, an index of refraction modulation scatters the laser beam into the required direction. Very high efficiencies can be achieved in small devices. However, the scaling of conventional AO devices is impractical because of the large aperture requirements, and the necessity of maintaining a uniform and high-power acoustic beam across the aperture. In addition, the requirements for generating the acoustic powers and the subsequent removal of the resulting heat in the material are quite severe. The approach taken at Rockwell uses the inherent optical nonlinearities in several of the AO materials to enhance the overall efficiency of the device at moderate- to high-power optical levels. This enhancement will be in the form of substantially lower acoustic power requirements for a given efficiency, and these devices will be able to steer over a much wider range of angles.

In the nonlinear device, the actual beam steering is accomplished via nondegenerate two-wave mixing between the primary input beam and the fraction of the input beam which is weakly deflected from the acoustic seed beam (the Kerr-Bragg process). The nonlinear optical gratings which are produced are subsequently amplified in the two-wave mixing process, substantially enhancing the diffraction efficiency of the acoustic grating. This unique process allows the use of the basic AO processes for agile beam steering of high-energy beams, without the requirements for

supplying large acoustic powers over large apertures. It is then possible to have the important advantages of AO beam steering for SDI directed energy efforts without the need for high-power acoustic devices. These advantages include:

- High efficiency deflection (~ 100%) for high optical energies
- Large resolvable number of spots (N > 1000 for large apertures)
- Fast access times (~ μs/mm aperture)
- Random access

Similar arguments can also be given for nondegenerate, two-wave mixing effects. These "artificial" photorefractive effects can also be used for beam steering applications (however, unlike the photorefractive materials, Kerr-Bragg media are rapid in response, limited only by phonon lifetime). The Kerr-Bragg process may also be thought of as a transverse Stimulated Brillouin Scattering (SBS) process. The interaction between the scattered wave and the pump beam intensifies the acoustic modulation of the index of refraction, giving rise to greater diffraction efficiencies with more energy transferred to the steered beam.

Two geometries for the application of this concept to ROBS can be developed. The first approach is referred to as Kerr-Bragg steering and is shown in Fig. 1. It resembles the geometry of conventional acousto-optical beam deflectors. The second approach shown in Fig. 2 is referred to as Resonant Nondegenerate Two-Wave Mixing (RNTWM), and it resembles the geometry used in Two-Wave Mixing experiments pioneered at the Rockwell Science Center in the last several years.

Since both of these approaches rely upon nonlinear processes that develop the highest diffraction efficiencies at high power, we believe the development of techniques to optimize the nonlinear response of conventional materials will be required, thereby reducing the requirement for laser beams of high peak power. In particular, we propose to capitalize upon research to develop nonlinear materials that are created by phase transitions near a critical point.

In addition to beam deflection, control of the phase of the acoustic signal allows piston phase control of the diffracted beam. Thus, this single element provides both steering and phasing of subapertures. In principle, detailed control of the phase front of the acoustic transducer (through the use of a phased array transducer of sufficient resolution) also can be used to provide adaptive

wavefront control to correct aberrations generated elsewhere in the system. Conversely, accurate acoustic wavefront control will be required to preserve the quality of the laser beam.

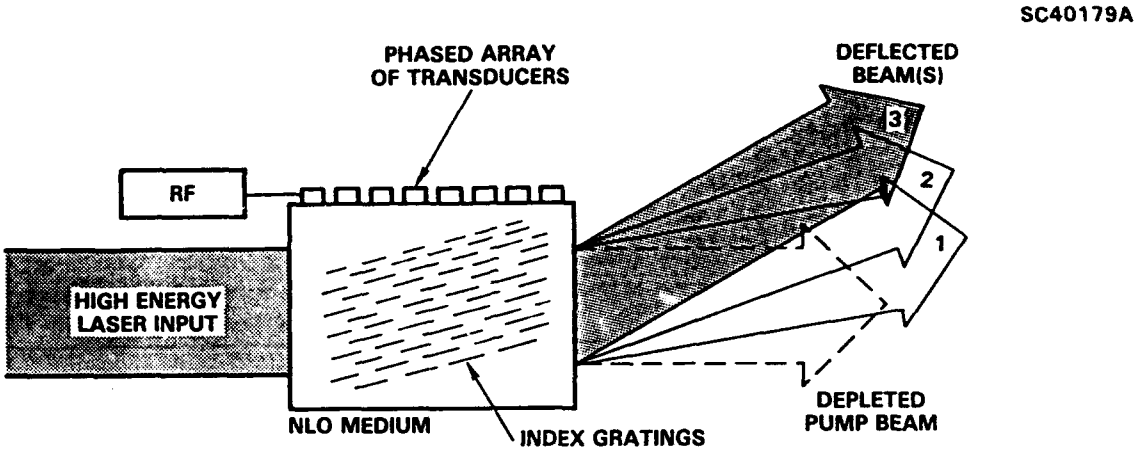

Fig. 1 Kerr-Bragg Steering.

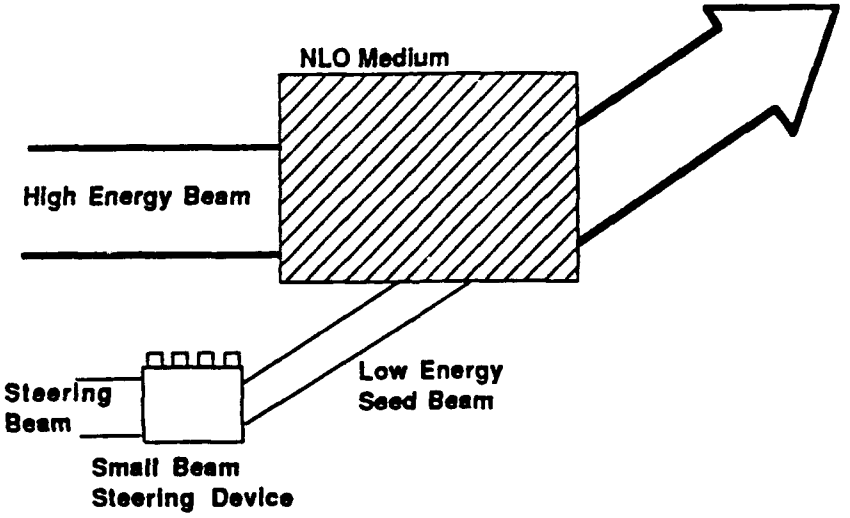

Fig. 2 Resonant Nondegenerate Two-Wave Mixing (RNTWM).

Beam Steering Criteria

The primary parameters of interest for beam steering devices are the number of resolvable spots N, the access time, and the efficiency of beam deflection. The maximum steering angle $\Delta\varphi$ is important for determining the resolution (N); however, $\Delta\varphi$ by itself is not very important since it can be changed by passive optics; e.g., lenses or mirrors. The resolvable number of spots are determined by the relation $N = \Delta\varphi/\Delta\beta$, where $\Delta\beta$ is the diffraction angle of the optical beam. For AO devices, it can be shown that $N = \Delta f\,\tau$, where Δf is the frequency bandwidth of the device, and τ is the transit time of the acoustic beam across the optical aperture. τ is also the access time required to switch the beam deflection angle, since it is the time required for modification to the acoustic grating (i.e., a new steering direction) to propagate across the aperture. Therefore, systems which utilize smaller subapertures have an intrinsically faster response time.

Kerr-Bragg Beam Steering

Conventional acousto-optical deflectors require approximately 1 W of RF power to reach high diffraction efficiency for a beam of approximately 1 mm diameter. For beams that are centimeters to meters in diameter, the power requirements can reach many kilowatts. This large power requirement is the fundamental limitation of conventional AO deflectors.

The Kerr-Bragg effect can be thought of as transverse SBS seeded by an acoustic wave launched at the correct phase-matching conditions. If the intensity of the input beam is sufficient to nearly reach the threshold for transverse SBS, the amplification of acoustic power by transverse SBS is exponential and can be very large. Since nonlinear optical Bragg scattering provides gain to the acoustic wave, the acoustic power required from the transducers is reduced by exp(gIL), where g is the nonlinear coupling constant or gain, I is the laser intensity, and L is the transverse interaction length. The power for the acoustic deflection is provided by the high-energy input laser beam; i.e., in a real sense the laser beam deflects itself. The input acoustic wave must have an intensity sufficiently above the noise level so that it can define the direction of stimulated scattering. In conventional SBS, the direction of scattering is in the direction with the greatest g IL product. The amplified seed beam must dominate the amplified spontaneous noise in order to control the transverse SBS process. For example, the threshold for SBS, which is mediated by the amplification of noise phonons, occurs for a g IL product of approximately 25. Therefore, gain approaching 100 dB is thought to be achievable with the proper geometry.

In addition to intensity, laser pulse length affects the gain of Kerr-Bragg processes. Theory predicts that the gain for transverse SBS should increase appreciably for near-forward angles with pulse lengths approaching microseconds in duration. The impact of higher gain for transverse SBS is a reduction of power required for lasers of long-pulse length compared with backwards SBS. It also should be noted that the acoustic transducers can be operated in a pulsed manner for use with a pulsed laser, giving further reductions in average power. If the laser pulse consists of a mode-locked pulse train where each pulse is of sub-nanosecond duration, it has been shown that the response to the sum of the individual mode-locked pulses is similar to a long continuous pulse in SBS.

The spectral width of the pulse also affects SBS gain. Extremely coherent but chirped pulses characteristic of radar pulses will require study in this program. Rocketdyne studies of "broadband" excimer emission have shown that the output consists of chirped narrow line emission and that this emission has a low SBS threshold consistent with narrow line emission as long as the chirp rate is less than the phonon lifetime.

Locking of SBS by injection of optical beams has been demonstrated. Acoustic seeding should provide an improved source for locking the scattered (deflected) beam to the input beam. The potential for high nonlinear gain implies a reduction of acoustic power from kilowatts to milliwatts for the same diffraction efficiency. The acoustic power in this technique is provided by power derived from the laser beam, that is, the optical interaction drives the generation of acoustic waves.

Preliminary experiments presented later in this section have shown an enhancement of diffraction efficiency with a small pulsed laser. Quartz was used as the AO material in this device. Other AO materials have a figure of merit orders of magnitude higher, and phase transition materials offer the possibility of further increases of several orders of magnitude.

Rapid Optical Beam Steering (ROBS) System Using Nonlinear Acousto-Optics

One of the most difficult technology development issues associated with laser radar is rapid optical beam steering (ROBS) of the laser beam. The technical challenge revolves around two central issues. The first challenge is the need for large beam steering angles—assumed to be on the order of 15 degrees. Second, these large angles must be addressed rapidly at retargeting times

assumed to be less than a millisecond. A large number of resolution elements is implied because these large angles must be addressed to a resolution within the diffraction limit of the output aperture.

It is recognized that a major reduction of the difficulty of this problem can be made by dividing the output aperture into a number of subapertures. The subapertures are phased and the phase between each subaperture is controlled in a manner similar to phased array radar to achieve beam steering. However, with optical radar, the limited diffraction from apertures of a reasonable size limits the beam steering angle of phased arrays to very small angles unless the subaperture elements are themselves steered. The problem is thus reduced to the ganged steering of a few hundred subapertures. Each subaperture, assumed to be of the order of 10 cm in size, must be able to address a number of resolution elements consistent with the total angle divided by the diffraction-limited beam divergence angle of the subaperture—a number of resolution elements assumed to be of the order of 10,000 or more in each axis (at a wavelength of 1 μm).

A number of beam deflection technologies have been considered for this application and discarded as limited to lower performance than what ultimately may be desirable. In this program we propose the application of new principles of operation that are made possible by the emerging understanding of the application of nonlinear optics to the control of beam phase and energy. Examples of these techniques are Stimulated Brillouin Scattering (SBS) for optical phase conjugation and Two-Wave Mixing (TWM) or the "photorefractive effect" for energy transfer.

The Rockwell Science Center (RSC) has been studying a process referred to as Resonant Nondegenerate Two-Wave Mixing (RNTWM) for use with "artificial photorefractors". Rocketdyne has been studying SBS for the beam control of large high power lasers. We believe there is an underlying fundamental relation between these two processes, since they can both be thought of as acoustically aided nonlinear processes. In a similar manner, these nonlinear processes are related to the acousto-optic processes that are used for AO beam deflectors and modulators.

These acoustically mediated nonlinear processes have the potential of providing direct electronic control of beam deflection with performance at least of the level discussed above. This proposal aims to demonstrate that these processes can achieve performance over a large subaperture with high efficiency and low power consumption.

A conceptual system configuration using the techniques that are to be developed in this program is shown in Fig. 3. The deflection system is a modular transmissive device that is located at the output of the laser system. The beam deflection module consists of an acoustic transducer coupled to a high efficiency nonlinear medium. The acoustic transducer is shown in this system as a two-dimensional array for addressing two axes of beam deflection. The nonlinear medium can be a fluid contained in a pressure cell. (A special material in this category was studied and developed at Rocketdyne, under a Navy contract.)

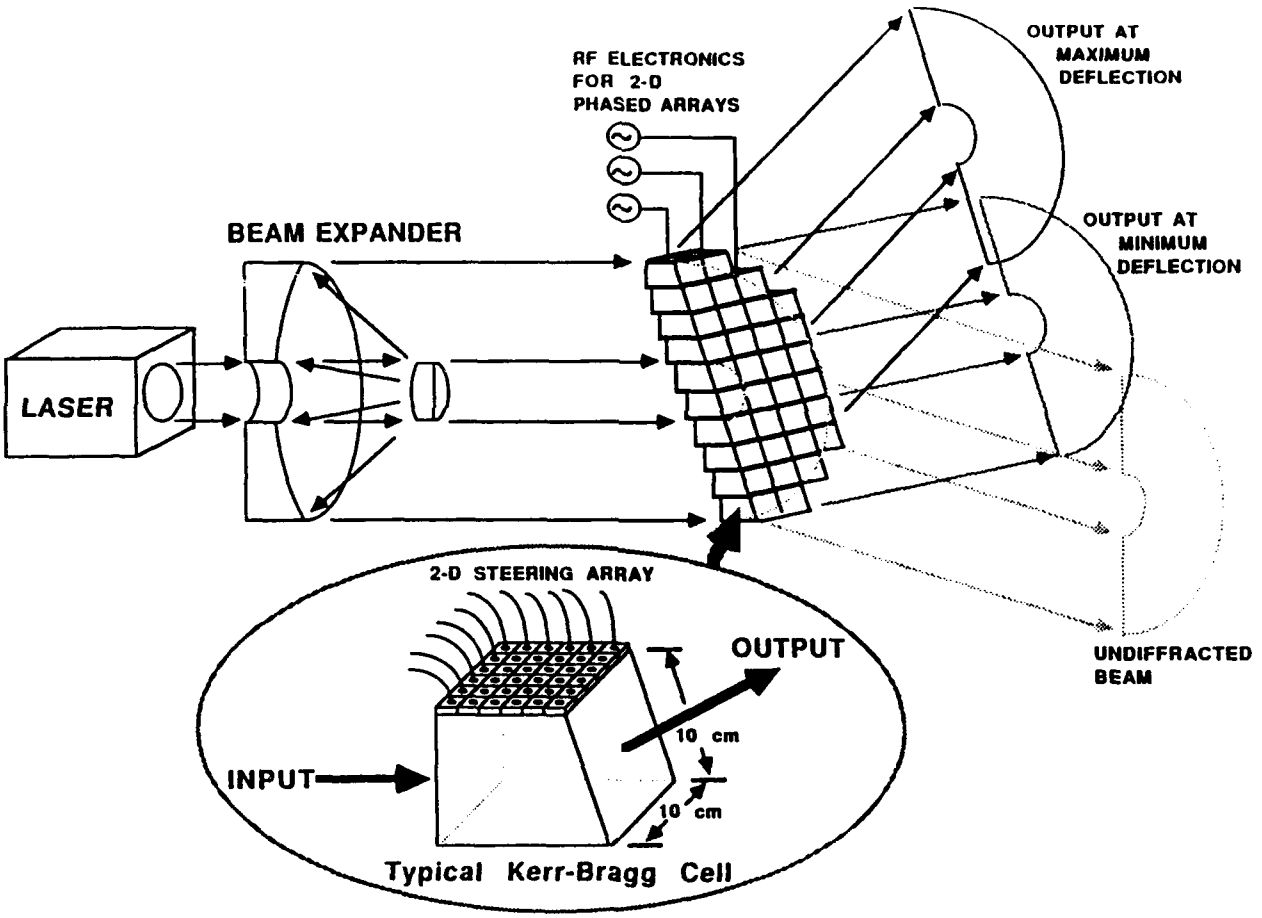

Fig. 3 Conceptual approach to a ROBS system based on nonlinear acousto-optics.

There are several interpretations or viewpoints that can be used to describe this beam deflection concept. The nonlinear energy exchange process for transferring (or scattering) light from the input beam to the deflected beam is referred to as Resonant Nondegenerate Two-Wave Mixing (RNTWM). This process can be thought of as analogous to TWM in an "artificial" photorefractive medium. In this medium, energy is transferred by diffraction from the input beam to a slightly downshifted and deflected beam. The redshift in the deflected beam establishes the

conditions necessary for preferential scatter of energy into the deflected beam with nonlinear (exponential) amplification.

This amplification allows the use of a very weak acoustic beam to initiate the diffraction of light. This weakly diffracted beam establishes a weak beam of light traveling in the correct direction. Through the nonlinear gain process this weak beam is rapidly (exponentially) amplified to high intensity. This process also can be thought of as acoustically seeded transverse Stimulated Brillouin Scattering (SBS). The transverse SBS generates acoustic waves traveling at the Bragg condition for scattering light transversely out of the beam. The SBS-generated acoustic wave greatly amplifies the transducer-generated acoustic wave, and this intensifies the optical scattered wave in a feedback process.

In summary, we can utilize the Kerr-Bragg effect to achieve the performance required for Rapid Optical Beam Steering (ROBS) mission(s). The nonlinear medium to be utilized was developed at Rocketdyne under a Navy contract for a broad range of nonlinear optics applications. In this application, unique material properties of the media result in high resolution and large deflection angle range with modest acoustic driving frequency power.